Journal of Pain Research

Dovepress
Taylor & Francis Group

Open Access Full Text Article

ORIGINAL RESEARCH

Metabolomics Analysis Reveals Gut Microbiota-Associated Sakuranin Modulates Endometrial Stem Cell Differentiation and Inflammation to Alleviate Pain in Endometriosis

Wen Shi[1–3,*], Minyi Wang[1–3,*], Zhuang Jin[1–3], Xiaochuan Chen[1–3], Jinbo Li[1–3], Huiling Lai[1–3], Xiao Li[1–3], Qiyu Zhong[1–3], Ye Chen[1–3], Shuqin Chen[1–3]

[1]Department of Gynecology, The Sixth Affiliated Hospital, Sun Yat-sen University, Guangzhou, Guangdong, People's Republic of China; [2]Key Laboratory of Human Microbiome and Chronic Diseases (Sun Yat-sen University), Ministry of Education, Guangzhou, Guangdong, People's Republic of China; [3]Biomedical Innovation Center, The Sixth Affiliated Hospital, Sun Yat-sen University, Guangzhou, Guangdong, People's Republic of China

*These authors contributed equally to this work

Correspondence: Shuqin Chen, Department of Gynecology, Block B, 12th Floor, Building 1, The Sixth Affiliated Hospital of Sun Yat-sen University, No. 26, Yuancun Erheng Road, Tianhe District, Guangzhou, Guangdong, 510655, People's Republic of China, Tel +86 13825039699, Email chshqin@mail.sysu.edu.cn

Background: Endometriosis (EMS) is characterized by pain symptoms that seriously affect patients' quality of life. Gut microbiome-related metabolites (GMRM) play an important role in the process of EMS. However, the role of GMRM in endometrial stem cells and EMS-related pain remains unclear.

Methods: An untargeted metabolomics approach was employed to analyze the fecal samples of 10 healthy individuals (heal), 11 EMS patients without dysmenorrhea (pless), and 14 EMS patients with dysmenorrhea (pain). The impact of potential key metabolite sakuranin on EMS-related pain was further investigated in vitro and in vivo.

Results: We identified 33 metabolites that were commonly changed in the painful group compared to the health and pless groups, and these metabolites were associated with differential microorganisms. Among them, sakuranin was downregulated in the painful group and exhibited a notably inverse correlation with the degree of pain. ROC curve revealed that sakuranin had a relatively high predictive value for EMS-related pain (AUC=0.8027). Functionally, sakuranin inhibited differentiation, migration, and inflammatory cytokine production, and decreased the expression of VEGF and ALCAM in SUSD2-positive primary endometrial cells. In EMS mice, sakuranin suppressed ectopic lesion growth, reduced inflammation, modulated angiogenesis and proliferation markers (VEGF, ALCAM, Ki-67), and regulated sympathetic and sensory nerve markers, resulting in alleviated pain behaviors.

Conclusion: We delineated the metabolic landscape related to EMS-related pain and uncovered that sakuranin has the potential to inhibit the growth of EMS and alleviate EMS-related pain. This finding offers therapeutic strategies of sakuranin in alleviating the pain symptoms associated with EMS.

Keywords: endometriosis, endometriosis-related pain, gut microbiome, metabolomics, sakuranin

Introduction

Endometriosis (EMS), a common and complex clinical entity characterized by the abnormal proliferation of endometrial tissue outside the uterus, is a pathological state responsive to estrogen that primarily leads to pelvic inflammation and potentially affects important reproductive organs such as the ovaries.[1] Chronic inflammatory diseases resulting from EMS are frequently accompanied by pain symptoms such as dysmenorrhea, pelvic pain, and dyspareunia.[2,3] The ectopic tissue in EMS can develop its own autonomic and sensory innervation. When mechanical stimulation is applied to the lesion, an increase in sensory nerve response can be observed, causing patients to experience pain upon mechanical

https://doi.org/10.2147/JPR.S557430
Received: 18 August 2025
Accepted: 20 January 2026
Published: 17 February 2026

stimulation.[4–6] The emergence of pain symptoms in EMS is associated with activating macrophages and mast cells, initiating a persistent cycle involving inflammation, and oxidative stress.[7–9] While the pain is rooted in endometrial lesions, its clinical presentation is often linked to neuroinflammation, angiogenesis, and sensitization processes.[10] Despite this, the underlying pathological mechanisms of EMS remain incompletely understood. In the clinical management of EMS-related pain, both hormonal and non-hormonal therapies play a critical role. However, current pharmacological interventions are either limited in efficacy or associated with adverse effects.[11,12] Consequently, elucidating the molecular mechanisms underlying pain in EMS is imperative for uncovering novel therapeutic approaches and enhancing the quality of life for patients with EMS.

Endometrial stem cells (EnSCs) are central to the understanding of EMS as a stem cell-related disease. During menstruation, poorly differentiated endometrial cells that shed may be the origin of primary endometrial lesions.[13–15] Studies reveal that during menstruation, cells or tissues with stem cell characteristics may detach from the basal layer of the endometrium.[13] Notably, SUSD2 is a well-established marker used to enrich endometrial mesenchymal stem/stromal cells, with $SUSD2^+$ cells predominantly residing in perivascular regions and exhibiting typical stem/progenitor properties.[16] Once the EnSCs abnormally migrate to sites like the pelvic peritoneum and ovaries, they can form ectopic foci via multiple pathways, such as epithelial-mesenchymal transition (EMT) and vascular or lymphatic channel metastasis. In the ectopic foci, EnSCs may abnormally differentiate, resulting in the formation of tissue structures like the endometrium at ectopic sites. This then causes menstrual cyclic bleeding and triggers inflammatory reactions and pain.[17] Data suggest that the invasive and angiogenic abilities of ectopic EnSCs are enhanced in vivo.[18,19] These cells boost the migratory, proliferative, and invasive abilities of ectopic EnSCs by upregulating the expressions of toll-like receptors, collectins, pro-inflammatory factors, and factors related to migration and angiogenesis.[20,21] However, the key mediators that govern the abnormal differentiation of EnSCs and their specific roles in EMS pain remain undefined.

EMS is regarded as a disease associated with the gut microbiota.[22] The gut microbiota may affect the occurrence and development of EMS through mechanisms such as influencing estrogen, immunity, inflammation, and tumor characteristics.[23] Metabolites from the gut microbiota are known to modulate host physiology. For instance, short-chain fatty acids, a type of microbial metabolite, have been shown to inhibit the growth of ectopic lesions in EMS.[24] A recent study in an EMS mouse model observed not only a decrease in intestinal flora diversity and abundance but also alterations in metabolite profiles. Notably, chenodeoxycholic acid and ursodeoxycholic acid levels increased significantly, while α-linolenic acid and 12,13-epoxy-9Z,11,15Z-octadecatrienoic acid (12,13-EOTrE) levels decreased.[25] However, the potential role of gut microbiome-related metabolites (GMRM) in EMS-associated pain remains unclear.

To search for the GMRM that can relieve EMS-related pain, we conducted untargeted metabolomics analyses on individuals with EMS who experience dysmenorrhea, those who do not, and healthy controls. We constructed a metabolic map related to EMS pain and conducted functional verification of the candidate key metabolite sakuranin in vivo and in vitro to explore its impact on the differentiation of EnSCs. This discovery elucidates a mechanism and offers a new treatment strategy for pain in EMS.

Materials and Methods

Study Population

Fecal samples were collected from 10 healthy volunteers and 25 EMS patients at the Sixth Affiliated Hospital of Sun Yat-sen University. Among the EMS patients, 14 had dysmenorrhea and 11 did not. Pain levels were assessed using the 11-point Numerical Rating Scale (NRS), where participants rated their pain intensity from 0 (no pain) to 10 (worst imaginable pain), allowing stratification of patients into dysmenorrhea and non-dysmenorrhea groups. All participants provided written informed consent, and this study was conducted in accordance with the Declaration of Helsinki. The study was conducted in compliance with ethical standards of medical research, with approval from the Ethics Committee of the Sixth Affiliated Hospital of Sun Yat-sen University (Approval No. 2024ZSLYEC-020). The specific inclusion and exclusion criteria of study participants for this study are as follows:

Inclusion criteria for the EMS patients were that the participants should be within the age range of 18 to 45 years; the diagnosis of ovarian endometriotic cysts should be confirmed by ultrasound or pelvic magnetic resonance imaging, which

has similar sensitivity and specificity (> 90%);[26] there should be no history of hormone therapy within the past 6 months; there should be no history of smoking; and there should be no other inflammatory or neuropathic pain disorders. Notably, given the clinical heterogeneity of endometriosis, this study specifically targeted the ovarian endometriotic cyst subtype for characterization. As most participants were outpatients who did not undergo surgery, r-ASRM staging could not be assessed.

Inclusion criteria for the control group were age 18–45 years; there should be no history of endometriosis; there should be no symptoms of dysmenorrhea; there should be no history of hormone therapy within the past 6 months; there should be no history of smoking; and there should be no other inflammatory or neuropathic pain disorders.

Exclusion criteria for the study were that there should be the presence of other pre-existing chronic abdominal diseases, kidney diseases, ovarian or uterine tumors, liver diseases, inflammatory or autoimmune diseases, and heart or coronary artery diseases; there should be receipt of hormone therapy within the 6 months before surgery; there should be long-term use of analgesic drugs; there should be a history of headaches or other neurological disorders; there should be discovery of severe pelvic inflammatory disease during the surgical procedure; there should be concurrent severe chronic or acute inflammatory diseases; and there should be co-occurrence of adenomyosis.

Metabolomics

Twenty-five milligrams of fecal samples were weighed and 300 μL of an extraction solution, prepared by mixing methanol and water in a 3:1 ratio, was added, ensuring thorough mixing. Subsequently, grind the samples at 35 Hz for 5 minutes to disrupt cell structures. Following this, the samples were placed in an ice-water bath and subjected to ultrasonic treatment for 5 minutes to extract intracellular components further. Then, the samples were incubated at −40 °C for 60 minutes to precipitate proteins. Once precipitation was complete, centrifuge the samples at 13,000 rpm for 15 minutes at 4 °C and collect the supernatant. Pool the supernatants from all samples in equal volumes to prepare a quality control sample set. The processed fecal samples were transferred into vials, after which Shanghai Majorbio Bio-Pharm Technology Co., Ltd. performed untargeted metabolomics analysis using their LC-MS/MS platform.

The analytical data were subjected to comprehensive processing and annotation using Progenesis QI software. For metabolite identification, the primary databases consulted were the Human Metabolome Database (HMDB, version 4.0), the METLIN database (version 1.0.6499.51447), public databases, and Majorbio's proprietary database. Subsequently, the *T*-test and orthogonal partial least-squares discrimination analysis (OPLS-DA) were applied to identify metabolites with significant differences. Permutation tests were conducted to ensure the robustness of the OPLS-DA model against overfitting. Cross-analysis was then used to determine the differential metabolites that were commonly regulated. To explore the functions and metabolic pathways associated with these metabolites, the Cluster of Orthologous Groups (COG) and Kyoto Encyclopedia of Genes and Genomes (KEGG) databases were utilized. The predictive potential of the differentially abundant metabolites was assessed using the receiver operating characteristic (ROC) curve analysis method. Finally, Spearman correlation analysis was used to analyze the differential metabolites and differential flora as well as the differential metabolites and clinical indicators and the differential microbiota (with $P < 0.05$).

Isolation, Culture, and Identification of Human Primary EnSCs

Human endometrial tissues were procured from patients undergoing hysteroscopic-laparoscopic surgeries for EMS. The tissues were thoroughly rinsed with normal saline and then dissected into 1 mm^2 pieces using sterile scissors. These fragments were subsequently placed into a digestion solution containing type IV collagenase, dispase, and DNase I, and incubated on a shaker at 50–70 rpm for 15–20 minutes. The digestion process was halted when single cells were observed to separate and glandular epithelial fragments became visible under microscopic examination. Cells were then filtered through a 40-micron sieve, and the resultant cells were incubated with magnetic beads conjugated to the Sushi Domain-containing 2 (SUSD2) antibody (PE anti-human SUSD2 Antibody, 327406, Biolegend). The SUSD2+ EnSCs were isolated using a magnetic separation technique (MojoSort Human anti-PE Nanobeads, 480091, Biolegend). The expression of SUSD2 on these endometrial stem cells was confirmed by immunofluorescence and flow cytometry. The cells were cultured in DMEM/F-12 medium supplemented with 10% fetal bovine serum (FBS) and 1% penicillin-streptomycin at 37 °C in an atmosphere containing 5% CO_2.

Flow Cytometry

We utilized flow cytometry to assess the expression of the marker SUSD2, thereby determining the identity of the isolated cells as EnSCs. Initially, 1×10^5 cells were incubated with the appropriately diluted SUSD2 antibody at 4 °C in a dark environment for 1 hour. Subsequently, the diluted goat anti-mouse IgG H&L was introduced, and the cells were further incubated at 4 °C in the dark for an additional hour. Following this, the cells were washed with PBS and resuspended in 200 μL of PBS for subsequent flow cytometric analysis (FACSVerseTM, BD).

Cell Counting Kit-8 (CCK-8) Cell Viability Assay

Cells were seeded into a 96-well plate at a density of 1×10^3 cells per well and allowed to adhere. After adhesion, the cells were exposed to various concentrations of sakuranin (0, 2, 4, 8, 16, and 32 μg/mL) for 48 hours. Subsequently, 10 μL of the CCK-8 reagent (C0038, Beyotime) was added into each well, and the cells were incubated for a further 2 hours. Upon completion of the incubation period, the optical density (OD) values at 450 nm were determined using a microplate reader (Infinite M1000, TECAN) to assess the cellular response to the treatment.

Enzyme-Linked Immunosorbent Assay (ELISA)

Following the manufacturer's protocol, the levels of interleukin-1β (IL-1β) (ml098416, Mlbio), interleukin-6 (IL-6) (ml098430, Mlbio), and tumor necrosis factor-α (TNF-α) (ml002095, Mlbio) in both EnSCs and mouse serum were quantified using ELISA kits. The OD readings at 450 nm were recorded to assess the concentrations of these cytokines.

Real-Time Quantitative PCR (RT-qPCR)

Total RNA was extracted from EnSCs and mouse serum using Trizol reagent (T9424, Sigma) and subsequently was reverse transcribed into cDNA with a reverse transcription kit (K1622, Thermo Fisher Scientific). Table 1 provides the forward and reverse primer sequences for epithelial cadherin (E-cadherin), cytokeratin 10, vimentin, neural cadherin (N-cadherin), and the internal reference gene, GAPDH. Subsequently, the synthesized cDNA served as a template for RT-qPCR in a 96-well plate, strictly following the manufacturer's guidelines. The RT-qPCR data were analyzed quantitatively using the $2^{-\Delta\Delta}$Cq method, with normalization to the mRNA levels of GAPDH to assess the relative expression of the target genes.

Western Blot

Following cell collection, RIPA lysis buffer supplemented with protease inhibitors was added, and the cells were incubated on ice for 10 minutes with intermittent vortexing at 30-second intervals every 5 minutes to enhance lysis. The samples were then centrifuged at 12,000 g for 10 minutes at 4 °C. Then, the supernatants, which contained the total protein extracts, were collected. SDS-PAGE was performed to separate the proteins, which were subsequently transferred

Table 1 Primer Sequence Information

Target Gene	Primer Sequence (5′ - 3′)
Cytokeratin 10-F	TCCTACTTGGACAAAGTTCGGG
Cytokeratin 10-R	CCCCTGATGTGAGTTGCCA
E-cadherin-F	CTGGCGTCTGTAGGAAGGCA
E-cadherin-R	GGGCAGTAAGGGCTCTTTGAC
N-cadherin-F	GCGTGAAGGTTTGCCAGTGT
N-cadherin-R	CGGCGTTTCATCCATACCAC
Vimentin-F	GCAATCTTTCAGACAGGATGTTG
Vimentin-R	TTCCTCTTCGTGGAGTTTCTTCA
GAPDH-F	ACAACTTTGGTATCGTGGAAGG
GAPDH-R	GCCATCACGCCACAGTTTC

Notes: GAPDH was used as the internal reference gene to normalize the relative expression levels of target genes.

onto PVDF membranes using a wet transfer method. After the transfer, the membranes were blocked at room temperature for 2 hours before overnight incubation with primary antibodies, including VEGF (1:5000, 19003-1-AP, Proteintech); ALCAM (1:5000, 21972-1-AP, Proteintech); GAPDH (1:15000, 60004-1-lg, Proteintech) at 4 °C. This was followed by a 1 to 2-hour incubation with secondary antibodies (Goat Anti-Mouse IgG H&L, 1:5000, RGAM001, Proteintech; Goat Anti-Rabbit IgG H&L, 1:5000, RGAR001, Proteintech). Finally, an ECL luminescence detection reagent (A38554, Thermo Fisher Scientific) was applied for signal development, and a chemiluminescence imaging system was utilized to expose and capture the images.

Scratch Assay

EnSCs were cultured in 24-well plates and assigned to three groups: a blank control, an inflammatory group treated with 1 μg/mL lipopolysaccharide (LPS) (L8880, Solarbio) for 48 hours, and a sakuranin group where 8 μg/mL sakuranin was added post-LPS treatment for 48 hours. The LPS treatment was applied to mimic the inflammatory microenvironment. A vertical scratch was created in the center of each well using a 1000 μL pipette tip. Wells were then gently washed with PBS to remove debris and floating cells and replenished with serum-free medium. Photographs of the cell monolayer were taken at 0 hours and 24 hours post-scratch to assess cell migration and wound closure. Quantitative analysis of the wound healing was performed using ImageJ software.

Immunofluorescence Staining

EnSCs were cultured in 24-well plates with the following experimental setups: a blank control, an inflammatory treatment with 1 μg/mL LPS for 48 hours, and a sakuranin treatment group where 8 μg/mL sakuranin was added post-LPS treatment for an additional 48 hours. Cells were fixed with 4% paraformaldehyde (P0099, Beyotime), permeabilized with 0.2% TritonX-100, and blocked with 3% bovine serum albumin (BSA). Antibody against SUSD2 (1:200) was incubated with the samples at 4 °C overnight in the dark. Cy3-labeled goat anti-mouse IgG (1:250, A0521, Beyotime) was then applied and incubated in the dark at room temperature for one hour. Nuclear staining was completed with DAPI. For cytoskeleton staining, after blocking with BSA, F-actin was stained with Actin-Tracker Green (C2201S, Beyotime) and then left to stand at room temperature for 1 hour. After being washed with PBS, the nuclei were stained with DAPI. Finally, the samples were observed under a fluorescence microscope (CKX53, Olympus).

The endometrial tissue of the sham group and the ectopic endometrial tissue of EMS mice were subjected to baking for deparaffinization and a subsequent hydration process. Antigen retrieval was then performed. Following a blocking step, the sections were incubated with diluted primary antibodies [Ki-67, 1:250, ab16667, Abcam; vascular endothelial growth factor (VEGF): 1:200, 19003-1-AP, Proteintech; activated leukocyte cell adhesion molecule (ALCAM), 1:200, 21972-1-AP, Proteintech; Cluster of differentiation 146 (CD146), 1:500, 17564-1-AP, Proteintech] at room temperature in the dark for 30 minutes. Afterward, Fluorescent secondary antibodies (B029, Ebiogo) were applied, and the samples were further incubated at room temperature in the dark for an additional 30 minutes. During pain-related biomarker assessment in tissue sections, tyrosine hydroxylase (TH) and Substance P (SP) were applied as markers of sympathetic and sensory nerve fibers. Their established roles in pain transmission make TH and SP reliable molecular indicators of EMS-associated pain.[27,28] Immunofluorescence double staining entails distinct procedures following blocking. Once blocking was completed, the TH antibody (1:200, 25859-1-AP, Proteintech) was added and incubated at room temperature for 30 minutes. After washing with PBS, a secondary antibody labeled with horseradish peroxidase (B001, Ebiogo) was introduced. Following another wash, the TSA fluorescent dye (Opal 520, EP1487001KT, AKOYA) was added and incubated for 10 minutes. Subsequently, the samples undergo antigen retrieval once again, and then the SP antibody (1:200, 20064, Immunostar) was added. After adding the secondary antibody and washing, the TSA chromogenic agent (Opal 570, EP1488001KT, AKOYA) was added. Hydrogen peroxide was dropped onto the samples and incubated at room temperature in the dark for 10 minutes to terminate the reaction. After terminating the reaction, the nuclei were counterstained with DAPI (C1006, Beyotime). Finally, the fluorescent sections were scanned using a digital slide scanner (3DHISTECH, Pannoramic MIDI).

Animal Study

All animal experiments in this study were approved by the Ethics Committee of the Sixth Affiliated Hospital of Sun Yat-sen University. All animal experiments were performed in accordance with the National Institutes of Health Guide for the Care and Use of Laboratory Animals. According to the method described by Lu et al,[29] we established the mouse model of EMS. We selected 28 female BALB/c mice (Spfbiotech, China) aged 4 to 8 weeks. The mice were housed in a specific pathogen-free laboratory center under a standard 12-hour light/12-hour dark cycle, with free access to food and water. Before the experiment, the mice underwent a one-week acclimatization period to stabilize their conditions. Eight donor mice received an intraperitoneal injection of 3 μg of estradiol (HY-B0141R, MCE) to stimulate endometrial growth. Three days post-injection, the donor mice were euthanized via carbon dioxide asphyxiation, and their uteri were excised and cut into fragments smaller than 1 mm^2. Each recipient mouse was then implanted intraperitoneally with 300 μL of normal saline containing the uterine fragments. On the day of the modeling injection, the recipient mice received another intraperitoneal injection of 3 μg of estradiol to promote the growth of ectopic lesions. A sham operation control group was also established, which received only 300 μL of normal saline intraperitoneally. Fourteen days later, the model was successfully established.

The mice were divided into four groups (n = 5): a sham operation control group, an EMS group, an EMS + Mixed Antibiotics treatment group, and an EMS + Mixed Antibiotics + Sakuranin treatment group. Previous studies have shown that antibiotics reduce lesion growth and inflammation in EMS models.[29–31] In this study, antibiotics were used to deplete gut microbiota, minimizing microbial interference in sakuranin metabolism and allowing precise assessment of its effects on EnSC differentiation and EMS-related pain. The sham operation control group received an equal volume of phosphate-buffered saline (PBS) via intraperitoneal injection under standard housing conditions. The EMS group, with a confirmed EMS model, was also maintained under standard conditions and received PBS injections. The EMS + Mixed Antibiotics treatment group was given a broad-spectrum antibiotic mixture (1 mg/mL of kanamycin sulfate, 0.07 mg/mL of gentamicin, 0.1135 mg/mL of polymyxin B sulfate, 0.43 mg/mL of metronidazole, 0.09 mg/mL of vancomycin) instead of drinking water for 7 days before the establishment of the EMS model, followed by sterile water to eliminate gut microbiota, and they also received PBS injections. The EMS + Mixed Antibiotics + Sakuranin treatment group, with depleted gut microbiota due to the antibiotic mixture, was administered sakuranin (HY-N3006, MCE) at a dose of 80 mg/kg via intraperitoneal injection after 14 days of endometrial tissue injection. Each group received its respective reagents once a week. After 28 days, the mice were weighed and then sacrificed. The ectopic lesions, serum, and peritoneal lavage fluid were collected for subsequent experiments.

Writhing Response

Following the establishment of the EMS model, on days 0, 7, 14, 21, and 28, mice were administered an intraperitoneal injection of oxytocin (HY-17571A, MCE) at a dosage of 0.3 mg/kg. The writhing responses were monitored and recorded within 30 minutes post-injection to assess pain-related behavior. The frequency of writhing episodes was documented for analysis of pain behavior. On the 28th day of model establishment, after recording the final body weights of the mice, they were humanely euthanized and dissected. Subsequently, mice were dissected to collect ectopic endometrial lesion tissues. Concurrently, serum and peritoneal lavage fluid were also retrieved for further analysis.

Statistical Analysis

This study performed statistical difference analysis using GraphPad Prism 9. The normality test and the homogeneity of variance were employed to ensure that the data met the prerequisites for statistical tests. To ensure the reliability of the experimental results, all experiments were repeated at least three times. When comparing two independent sample groups, an unpaired independent-sample *t*-test was conducted; for data that did not conform to normal distribution or had unequal variances, the Mann–Whitney test was employed. When evaluating the differences among three or more groups, one-way ANOVA (analysis of variance) followed by Tukey's test was adopted. The Kruskal–Wallis test was used if the data distribution did not conform to the normal distribution. Fisher's exact test was used for the data that were categorical and had a limited sample size. The results were considered statistically significant when the statistical parameter P-value was less than 0.05.

Results

Characteristics of the Participants in this Study

The clinical characteristics of the study participants are detailed in Table 2. The study cohort comprised 35 individuals, including 14 patients with EMS accompanied by dysmenorrhea (mean age, 30.39 years), 11 patients without dysmenorrhea (mean age, 29.18 years), and 10 healthy controls (mean age, 28.4 years). Comparative analyses among the groups revealed no significant differences in age, body mass index (BMI; $P>0.05$), or age at menarche (AAM; $P>0.05$). The volume of ovarian endometrioma (VOE) did not show significant differences between the EMS groups ($P>0.05$). In both EMS groups, unilateral cysts were more prevalent than bilateral cysts ($P<0.001$). Serum CA125 levels differed significantly across groups ($P=0.004$), whereas anti-Müllerian hormone (AMH; $P=0.183$), carbohydrate antigen 19–9 (CA19-9; $P=0.082$), and the neutrophil-to-lymphocyte ratio (NLR; $P=0.479$) showed no significant differences. In summary, the EMS with dysmenorrhea group was distinguished by elevated pain severity, prolonged pain duration, and higher CA125 levels, while demographic and most inflammatory markers remained comparable across groups.

Comprehensive Metabolomics Profile of Patients with EMS-Related Pain

To elucidate the metabolomic profile associated with EMS pain, we performed untargeted metabolomics using fecal samples from 10 healthy individuals (heal), 11 EMS patients without dysmenorrhea (pless), and 14 EMS patients with dysmenorrhea (pain). The metabolomics analysis revealed 17,233 metabolite peaks, comprising 7,265 positive and 9,968 negative ion metabolites. Rigorous quality control was applied to the raw data, with the relative standard deviation (RSD) below 30% and the cumulative peak proportion over 70%, ensuring data quality (Figure S1A). Correlation analysis using the Pearson correlation coefficient on 35 samples revealed a high correlation among samples within the same group, confirming sample reproducibility (Figure S1B).

Table 2 Characteristics of the Study Participants

Characteristics	Control	EMS without Dysmenorrhea	EMS with Dysmenorrhea	*P* value
n	10	11	14	–
Age, years	28.4±4.55	29.18±4.47	30.93±5.73	0.456[a]
BMI	21.16±2.71	19.53±1.55	19.38±2.05	0.112[a]
Pain level	–	–	5.39±2.39	–
AAM, years	13.5±1.08	13±0.77	12.86 ±1.41	0.279
Pain = yes n (%)	0 (0.0)	0 (0.0)	14 (100.0)	**<0.0001**[b]
Gravidity	0 (0, 1)	0 (0, 1)	0 (0, 1)	–
Parity	0 (0, 0)	0 (0, 0)	0 (0, 1)	–
Number of miscarriages	0 (0, 0)	0 (0, 0)	0 (0, 0)	–
VOE, mm^3	–	80,659.22±74,255.06	55,441.67±103,224.35	0.182[c]
Unilateral/Bilateral Endometriotic Cysts (%)				**<0.001**[b]
Unilateral	0 (0.0)	9 (81.81)	10 (71.43)	–
Bilateral	0 (0.0)	2 (18.18)	4 (28.57)	–
None	10 (100.0)	0 (0.0)	0 (0.0)	–
Pain, years	–	–	7.43±5.50	–
AMH, ng/mL	4.70±1.25	3.94±2.35	3.23±1.82	0.183[a]
CA125, U/mL	21.27±16.16	43.87±37.26	76.06±53.07	**0.0004**
CA19-9, U/mL	10.45±8.01	16.64±14.60	31.71±38.29	0.082
N	3.69±1.28	4.52±2.05	3.63±0.89	0.523
L	2.16±0.79	2.13±0.61	1.76±0.58	0.361
NLR	1.81±0.63	2.18±0.83	2.31±1.11	0.479

Notes: Data are represented as mean ± standard deviation (SD) or medians and interquartile ranges. Data were statistically analyzed using Kruskal–Wallis test, with the exception of the data labeled as a, b, and c. [a]Indicates One-Way ANOVA tests, [b]indicates Fisher's exact test, and [c]indicates Mann–Whitney test. Statistically significant p-values are highlighted in bold.

Abbreviations: BMI, body mass index; AAM, age at menarche; VOE, volume of ovarian endometrioma; AMH, antimüllerian hormone; CA125, glycoconjugate antigen 125; CA19-9, glycoconjugate antigen 19–9; N, neutrophil; L, lymphocyte; NLR, neutrophil/lymphocyte ratio.

https://doi.org/10.2147/JPR.S557430

We constructed three OPLS-DA models to analyze comprehensive metabolite differences across three sample groups. To validate the models, we performed 200 permutation tests to assess their fit. The OPLS-DA models revealed distinct metabolic profiles among EMS patients and healthy controls. The model comparing EMS patients with dysmenorrhea to healthy controls showed an R2 intercept of 0.965 and a Q2 intercept of −0.0951 (Figure 1A and B). When contrasting EMS patients with dysmenorrhea to those without, the R2 intercept was 0.9938, with a Q2 intercept of −0.1282 (Figure 1C and D). Similarly, the metabolic differences between EMS patients without dysmenorrhea and healthy controls were marked, as evidenced by the R2 intercept of 0.989 and Q2 intercept of −0.016 (Figure 1E and F). All models demonstrated negative Q2 intercepts, indicating robust predictive ability and effective differentiation between groups.

Differential Metabolite Profiling in Endometriosis with and without Dysmenorrhea

To visually present differential metabolites, we utilized volcano plots for intuitive visualization and variable importance in projection (VIP) analysis to elucidate the significance and expression trends of differential metabolites (VIP > 1, $P < 0.05$) across the three groups. Compared with healthy controls, EMS patients with dysmenorrhea exhibited 140 upregulated and 66 downregulated metabolites (Figure 2A). VIP analysis revealed that roquefortine was upregulated, while sakuranin and sinapic acid 4-O-sulfate were downregulated in EMS patients with dysmenorrhea relative to healthy controls (Figure 2B). Compared to EMS patients without dysmenorrhea, those with dysmenorrhea exhibited 248 differential metabolites, with 137 upregulated and 111 downregulated in the dysmenorrhea group (Figure 2C). Notably, Z-PP-CHO and 7,8-Dihydroxycoumarin were upregulated in EMS patients with dysmenorrhea, and 23-trans -p-Coumaroyloxytormentic acid, 8-Hydroxyluteolin 8-sulfate, and phenylalanyl-prolyl-arginine were downregulated in EMS patients with dysmenorrhea compared to those without dysmenorrhea (Figure 2D). Between EMS patients without dysmenorrhea and healthy controls, 182 differential metabolites were identified, with 91 upregulated and 91 downregulated in EMS patients without dysmenorrhea (Figure 2E). DG (LTE4-13:00/0:00) was upregulated, and taurolithocholic acid 3-sulfate was downregulated in EMS patients without dysmenorrhea relative to healthy controls (Figure 2F).

KEGG Pathway Enrichment Analysis of Differential Metabolites

To further explore the key signaling pathways in which the differential metabolites are involved, this study analyzed the metabolic pathways related to these metabolites by leveraging the KEGG database. Differential metabolites between EMS patients with dysmenorrhea and healthy controls were enriched in multiple metabolic pathways, including benzoxazinoid biosynthesis, vitamin B6 metabolism, caffeine metabolism, histidine metabolism, and steroid biosynthesis (Figure S2A). A similar pattern was observed in the metabolite disparities between EMS patients with and without dysmenorrhea, with pathways such as betalain biosynthesis, pantothenate and CoA biosynthesis, and riboflavin metabolism being implicated (Figure S2B). Finally, the metabolite variations between EMS patients without dysmenorrhea and the healthy control group affected pathways including caffeine metabolism, caprolactam degradation, aminobenzoate degradation, and alpha-linolenic acid metabolism (Figure S2C).

Differential Metabolites are Correlated with Clinical Indicators

To further explore the potential associations between differential metabolites and clinical indicators, we analyzed the correlations between the differential metabolites and clinical indicators such as patient's age, BMI, pain level, AAM, the volume of VOE, AMH, CA125, CA19-9, N, L, and NLR. In the comparison between EMS patients with dysmenorrhea and healthy controls, sakuranin, ketamine, taurolithocholic acid 3-sulfate, among others, showed significant negative correlations with pain level ($P < 0.05$), whereas allopregnanolone, neocnidilide, and 2,2-Dimethyl-5-hydroxy-1-pyrrolidinyloxy were positively correlated with pain ($P < 0.05$) (Figure S3A). For the differential metabolites between the EMS patients with dysmenorrhea and the group of EMS patients without dysmenorrhea, sakuranin, (S,S)-Butane -2,3-diol, 8-Hydroxyluteolin 8-sulfate, phenylalanyl-prolyl-arginine, etc. were the top metabolites with significant negative correlation to pain level ($P < 0.05$), and 6-(2-Hydroxyethoxy)-6-oxohexanoic acid, N-Formyl-L-glutamic acid, nigerloxin, etc. were the top significant positive correlation to pain level ($P < 0.05$) (Figure S3B). For the differential metabolites between the EMS patients without dysmenorrhea and the healthy control group, 4-O-Methylgallic acid, Methyl 2,4,6-trihydroxybenzoate, 6-Thiourate, etc. were the top significant negative correlation

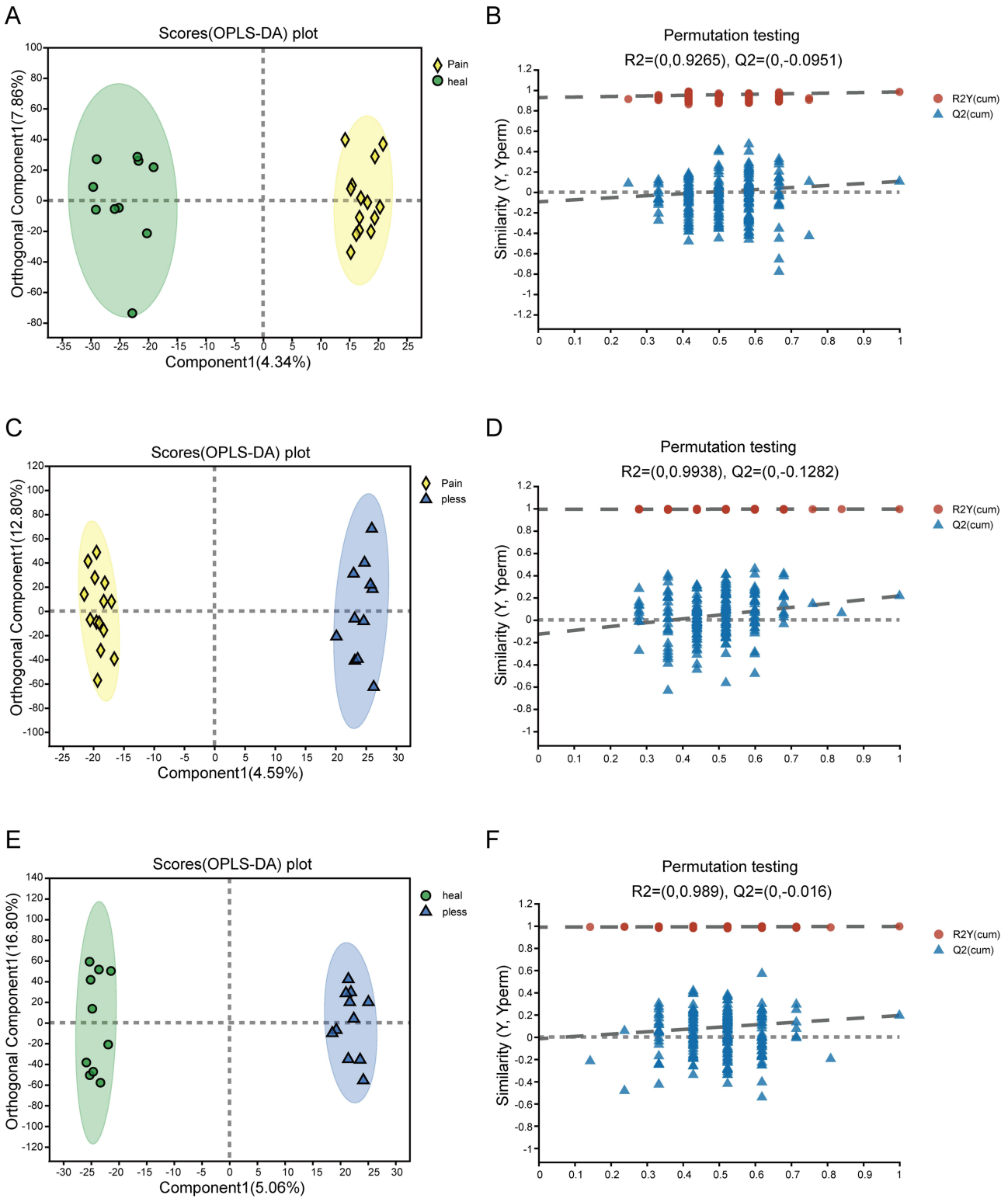

Figure 1 Orthogonal partial least squares discriminant analysis (OPLS-DA) model analysis. (**A** and **B**) OPLS-DA analysis between the pain group and the heal group; (**C** and **D**) OPLS-DA analysis between the pain group and the pless group; (**E** and **F**) OPLS-DA analysis between the heal group and the pless group. Pain group: Patients with endometriosis (EMS) accompanied by dysmenorrhea; pless group: Patients with EMS without dysmenorrhea; heal group: Healthy control group.

https://doi.org/10.2147/JPR.S557430

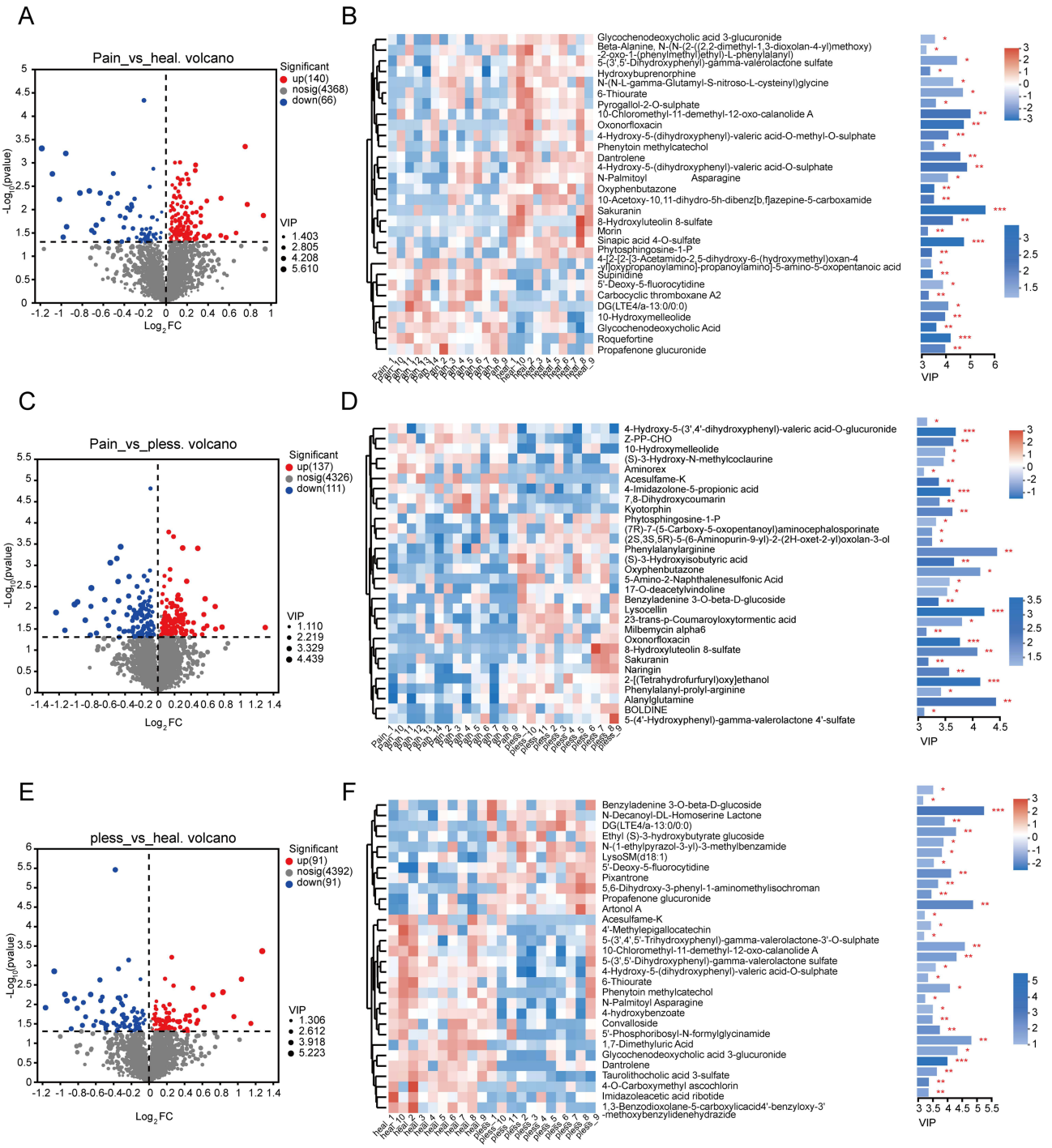

Figure 2 Analysis of differential metabolites among groups. (**A**) Volcano plot of differential metabolites between the pain group and the heal group; (**B**) Metabolite hierarchical clustering (left) and Variable Importance in Projection (VIP) score plot (right) comparing the pain group with the heal group; (**C**) Volcano plot of differential metabolites between the pain group and the pless group; (**D**) Metabolite hierarchical clustering (left) and VIP score plot (right) comparing the pain group with the pless group; (**E**) Volcano plot of differential metabolites between the pless group and the heal group; (**F**) Metabolite hierarchical clustering (left) and VIP score plot (right) comparing the pless group with the heal group. Pain group: Patients with EMS accompanied by dysmenorrhea; pless group: Patients with EMS without dysmenorrhea; heal group: Healthy control group. *P < 0.05, **P < 0.01, ***P < 0.001.

to NLR level, while (E,E)-Trichostachine, 4-Hydroxy-4-(3-pyridyl)-butanoic acid, Bucolome, etc. were the top significant positive correlation to NLR level (P < 0.05) (Figure S3C). Our results demonstrate that certain gut microbiota–associated metabolites are closely correlated with EMS-associated pain and systemic inflammatory status.

The Key Metabolite - Sakuranin is Negatively Correlated with the Pain of EMS

In our previous study, we performed a microbiome analysis on the feces of volunteers.[32] To further explore the GMRM, we examined the potential associations between the differential metabolites and differential microbiota at the genus level via Spearman correlation analysis. For EMS patients with dysmenorrhea versus healthy controls, correlations between 206 differential metabolites and 11 differential microbial genera were analyzed. The results showed that the metabolite flavogallol was significantly positively correlated with Prevotella (Table S1; Figure S4A). For the group of EMS patients with dysmenorrhea and the group of EMS patients without dysmenorrhea, the correlation between 248 differential metabolites and 11 microbes was analyzed. It was found that the metabolite diphenhydramine N-glucuronide was significantly negatively correlated with Faecalibacterium, and (2S)-5-Oxopyrrolidine-2-carbaldehyde was significantly positively correlated with Lachnospiraceae_UCG_004 (Table S2; Figure S4B). When comparing the healthy control group with the group of EMS patients without dysmenorrhea, the correlation between 182 differential metabolites and 16 microbes was analyzed. It was discovered that the metabolite Inosine, 2′,3′-dideoxy - was significantly positively correlated with Roseburia, and Flavogallol was significantly negatively correlated with Bifidobacterium (Table S3; Figure S4C). Differential microbes correlated with differential metabolites.

To identify the important metabolites closely related to pain and the gut microbiota, we first screened out the microbes and metabolites that were co-upregulated or co-downregulated in the two comparisons of "EMS with dysmenorrhea group vs healthy control group" and "EMS with dysmenorrhea group vs EMS without dysmenorrhea group". After identifying the commonalities between the two comparisons, 33 commonly regulated differential metabolites and 43 commonly differential microbes at the species level were obtained (Figure 3A and B). A Spearman correlation analysis was conducted on the 33 differential metabolites and 43 differential microbes to further explore the potential connection between these metabolites and microbes (Figure 3C). The results indicated that the differential metabolites and microorganisms exhibited varying degrees of correlation.

In addition, a clustering analysis was carried out on the expression patterns of 1,726 metabolites, which were divided into 9 different expression patterns (Figure S5), we focused on cluster 9, because its level was highest in the healthy control group, decreased in the EMS without dysmenorrhea group, and was lowest in the EMS with dysmenorrhea group. Then, we took the intersection of 33 differential metabolites and the metabolites in cluster 9, obtaining 11 differential metabolites (Figure 3D). We conducted the ROC analysis on these 11 metabolites, and the results showed that these metabolites had excellent predictive effects on EMS as well as pain (Figure S6). Furthermore, a Spearman correlation analysis was carried out on these 11 metabolites and various clinically relevant indicators. As expected, all 11 metabolites with down-regulated expression in the pain group were significantly negatively correlated with pain. CA125 can be used for diagnosing endometriosis. Although the sensitivity and specificity of CA125 are relatively low,[33] it remains a widely used biomarker for the diagnosis of endometriosis in clinical practice. Research findings have demonstrated that elevated blood CA125 levels bear statistical significance in patients suffering from chronic pelvic pain and dysmenorrhea.[34] Therefore, we further focused on the metabolites related to CA125 and found that sakuranin was the most significantly negatively correlated with CA125 (Figure 3E). Hence, we chose sakuranin for further research. Metabolomic analysis revealed the abundance of sakuranin (Figure 3F). Compared with healthy controls, sakuranin levels were reduced in EMS patients without dysmenorrhea and further decreased in those with dysmenorrhea, suggesting a negative association between sakuranin and the occurrence of dysmenorrhea in EMS. The scatter plot of the correlation between sakuranin and the degree of pain indicated a significant negative correlation between them ($P = 0.0033$) (Figure 3G). Subsequently, the ROC curve was employed to evaluate the predictive performance of sakuranin for EMS and pain. The results showed that sakuranin had a good predictive performance for EMS (area under the curve [AUC] = 0.728) (Figure 3H) and had an excellent predictive performance for whether EMS was accompanied by pain (AUC = 0.8027) (Figure 3I). In conclusion, sakuranin is downregulated in the pain group and exhibits a negative correlation with pain levels.

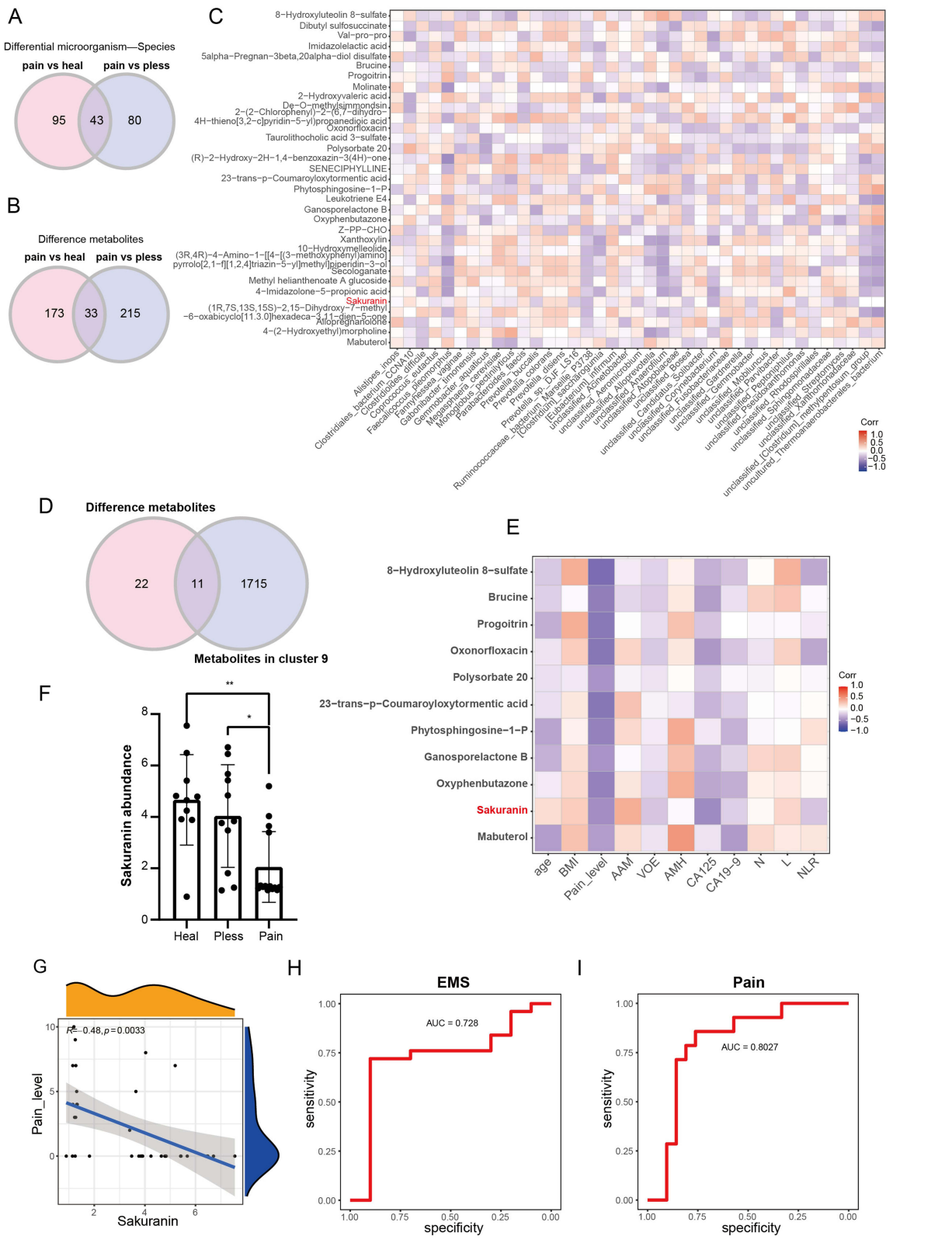

Figure 3 The metabolite sakuranin is negatively correlated with the pain of EMS. (**A**) Venn diagram for screening differential microbes at the species level between the pain vs heal and pain vs pless groups; (**B**) Venn diagram for screening differential metabolites between the pain vs heal and pain vs pless groups; (**C**) Correlation between differential metabolites and differential microbes; (**D**) Venn diagram for screening differential metabolites with the expression pattern of cluster 9; (**E**) Correlation analysis between differential metabolites and clinical indicators; (**F**) The content of sakuranin in the pain group, the pless group, and the heal group. The Y-axis represents the peak area ratio of sakuranin. The internal standards used in the experiment include L-2-Chlorophenylalanine, etc; (**G**) Scatter plot showing the negative correlation between sakuranin and pain level; (**H**) Receiver operating characteristic (ROC) analysis of sakuranin for EMS; (**I**) ROC analysis of sakuranin for pain. Pain group: Patients with EMS accompanied by dysmenorrhea; pless group: Patients with EMS without dysmenorrhea; heal group: Healthy control group. *$P < 0.05$, **$P < 0.01$.

Sakuranin Inhibits the Differentiation of EnSCs into Mesenchymal Cells and Reduces the Levels of Inflammatory Factors and Angiogenesis Markers

The isolated primary endometrial cells expressed SUSD2, a highly specific surface marker for endometrial epithelial stem/progenitor cells[16] (Figure 4A), with 90.40% ± 0.97% of cells being SUSD2-positive (Figure 4B). A concentration gradient of sakuranin (0–32 μg/mL) was used to determine the optimal concentration. Cell viability was assessed relative to the untreated control (0 μg/mL, set as 100%). Treatment with 8 μg/mL sakuranin for 48 hours showed low cytotoxicity to EnSCs, and this concentration was selected for subsequent experiments (Figure 4C).

EnSCs were treated with LPS to create an inflammatory environment and then sakuranin was administered. ELISA experiments were performed to analyze the inflammation-related cytokines in EnSCs. It was found that LPS significantly promoted the expression of IL-1β, IL-6, and TNF-α, while sakuranin significantly inhibited the secretion of these inflammatory factors (Figure 4D–F). Western blot was utilized to detect the expression levels of the angiogenesis markers ALCAM and VEGF in EnSCs. The results indicated that treatment with LPS significantly promoted the expression of ALCAM and VEGF in EnSCs, while sakuranin could reverse this response, making the protein expression levels of ALCAM and VEGF in the sakuranin-treated group lower than those in the LPS group (Figure 4G–I). RT-qPCR experiments were conducted to detect the expression of differentiation markers. The results showed that LPS suppresses the expression of epithelial cell markers E-cadherin and Cytokeratin 10 while promoting the expression of mesenchymal cell markers vimentin and N-cadherin, facilitating the transition of EnSCs towards a mesenchymal phenotype. However, sakuranin significantly reverses the LPS-induced EMT effects (Figure 4J–M). The structural changes of filamentous actin were observed by staining with fluorescein-labeled phalloidin. LPS led to an increase in the size of EnSCs, making them star-shaped and with their protrusions interconnected into a network structure. Treatment with sakuranin could alleviate such morphological changes in the cells (Figure 4N). The cell scratch assay showed that LPS significantly promoted the cell healing ability of EnSCs within 24 hours, while treatment with sakuranin significantly reduced the enhancement of the migratory ability of EnSCs caused by LPS (Figure 4O). In all, sakuranin shows significant inhibitory effects on LPS-induced inflammatory response, differentiation, and migratory ability of EnSCs.

Sakuranin Alleviates the Progression of EMS in Mice

To further verify the regulatory effect of sakuranin on the pain of EMS, a mouse EMS model was established and treated with antibiotics and sakuranin (Figure 5A). On the 28th day after the successful establishment of the model, the body weights of the mice were measured before euthanasia. There was no significant difference in body weight between the EMS model group and the sham group (Figure 5B and C). Compared with the model group, treatment with antibiotics alone or the combination of antibiotics and sakuranin could significantly inhibit the growth of ectopic endometrial lesions in mice (Figure 5D). Particularly, compared with EMS mice treated with antibiotics alone, the weight of endometrial lesions in mice treated with the combination of antibiotics and sakuranin was further reduced ($P = 0.0008$). Taken together, sakuranin can alleviate the progression of EMS lesion growth.

To explore the impact of sakuranin on the pain level of EMS, the number of writhing responses of mice was counted. The results showed that the number of writhing responses in EMS mice was much higher than that in the sham group. Using mixed antibiotics could reduce this behavior, and the treatment with sakuranin combined with mixed antibiotics could further alleviate the pain of EMS (Figure 5E). To verify the potential role of sakuranin in inflammatory response and the differentiation of EnSCs in EMS mice, ELISA and RT-qPCR were employed to detect the inflammatory factors and differentiation markers in the endometrial tissue of EMS mice. The ELISA results of the peritoneal fluid indicated that antibiotic treatment could significantly reduce the increased expression levels of the inflammatory factors IL-1β and TNF-α caused by EMS. Moreover, when sakuranin was combined with antibiotic treatment, sakuranin could further inhibit the expression of IL-1β and TNF-α (Figure 5F and G). RT-qPCR analyses revealed that in comparison to the sham group, the expression of epithelial markers (Cytokeratin 10 and E-cadherin) was significantly decreased, whereas the expression of mesenchymal markers (N-cadherin and vimentin) was markedly increased in EMS mice. Antibiotic intervention effectively reversed these alterations, and the addition of sakuranin to the antibiotic treatment could further enhance the effect (Figure 5H–K).

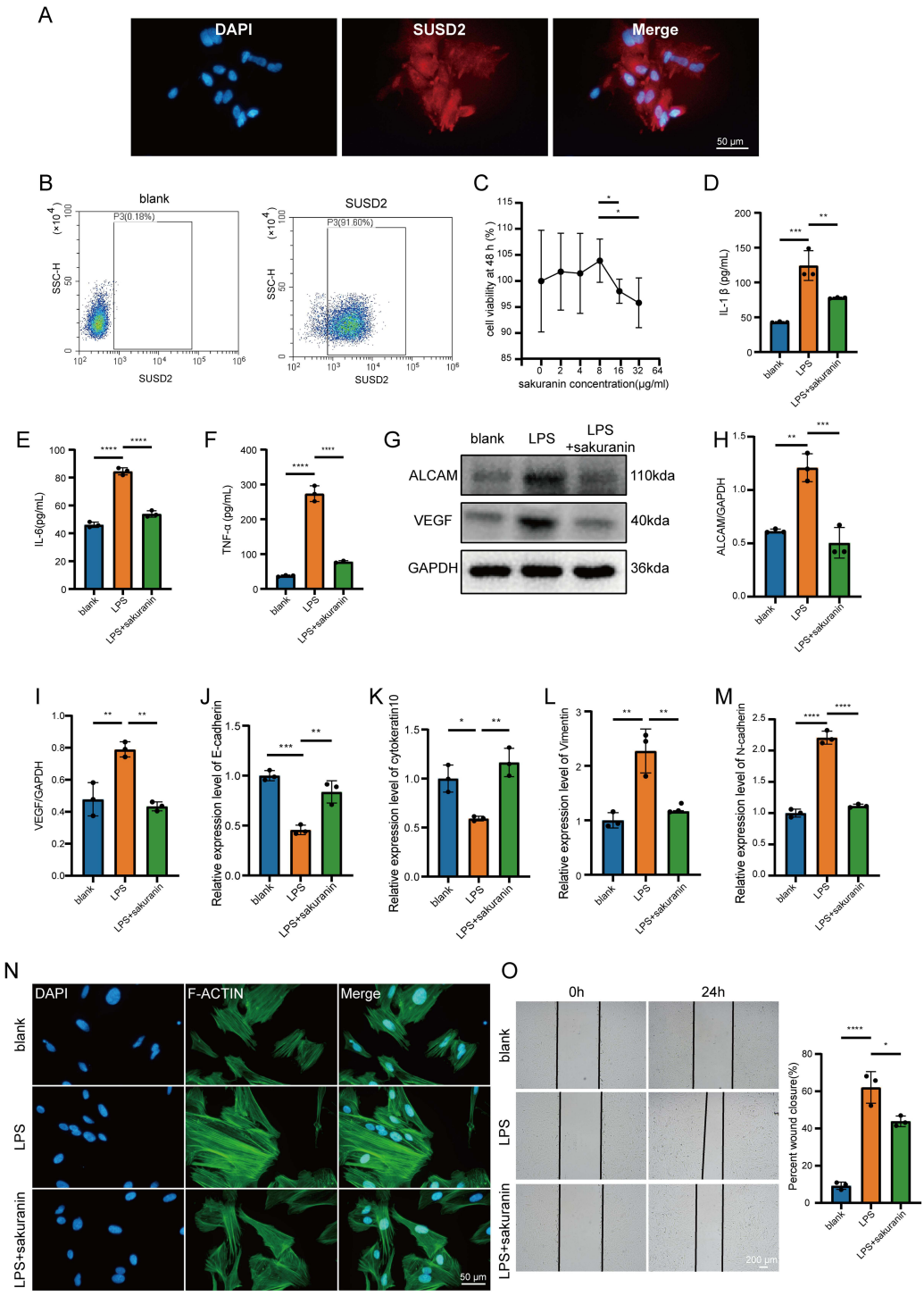

Figure 4 Sakuranin inhibits the differentiation of EnSCs into mesenchymal cells and reduces the levels of inflammatory factors. (**A**) The expression level of the Sushi Domain-containing 2 (SUSD2) protein in EnSCs. The expression of the SUSD2 protein is presented in red fluorescence, and the nuclear DAPI staining is shown in blue; (**B**) The flow cytometry scatter plot of EnSCs without treatment with the SUSD2 antibody (left) and of EnSCs incubated with the SUSD2 antibody (right); (**C**) Screening for the optimal concentration of sakuranin; (**D**–**F**) Detection of the contents of interleukin-1β (IL-1β), interleukin-6 (IL-6), and tumor necrosis factor-α (TNF-α) in EnSCs by enzyme-linked immunosorbent assay (ELISA); (**G**–**I**) Detection of the expression levels of the activated leukocyte cell adhesion molecule (ALCAM) and the vascular endothelial growth factor (VEGF) in EnSCs by Western blot and the quantitative analysis of protein expression; (**J**–**M**) Detection of the mRNA expressions of epithelial cadherin (E-cadherin), cytokeratin 10 (Cytokeratin 10), vimentin, and neural cadherin (N-cadherin) in human primary EnSCs by real-time quantitative polymerase chain reaction (RT-qPCR); (**N**) Phalloidin staining of the cytoskeleton of EnSCs. The green fluorescence represents phalloidin staining, and the blue fluorescence represents the counterstaining of the nucleus by DAPI; (**O**) Detection of the migratory ability by scratch assay and the quantitative analysis of the scratch healing of EnSCs. The cells were treated with 1 μg/mL lipopolysaccharide (LPS) for 48 hours. *$P < 0.05$, **$P < 0.01$, ***$P < 0.001$, ****$P < 0.0001$.

https://doi.org/10.2147/JPR.S557430

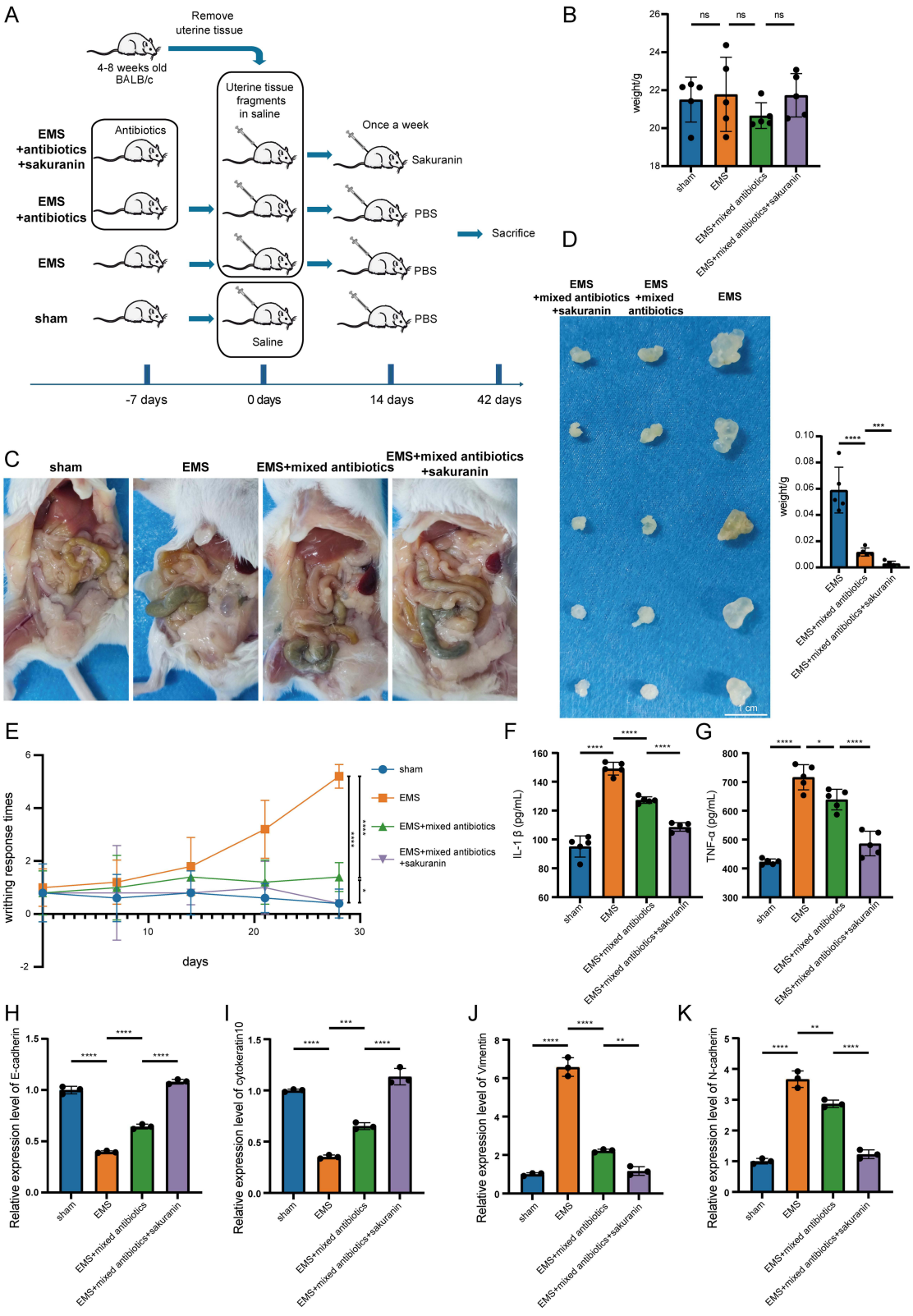

Figure 5 Sakuranin alleviates the progression of EMS. (**A**) Flow chart of the EMS mouse model construction; (**B**) Measurement of mice body weight; (**C**) Representative gross images of ectopic lesions from each group: the sham group, the EMS model group, the EMS group treated with antibiotics, and the EMS group treated with antibiotics-sakuranin; (**D**) Diagram of ectopic endometrial lesions in mice and measurement of the weight of ectopic endometrial lesions in mice. n = 5; (**E**) Influence of sakuranin on the writhing response of EMS mice; (**F** and **G**) Detection of the levels of IL-1β and TNF-α in the peritoneal fluid by ELISA. n = 5; (**H**–**K**) Detection of the expressions of E-cadherin, Cytokeratin10, vimentin, and N-cadherin in the endometrial tissue of the sham group and the ectopic endometrial tissue of EMS mice by RT-qPCR. n = 3, ns indicates no significance, **P* < 0.05, ***P* < 0.01, ****P* < 0.001, *****P* < 0.0001.

https://doi.org/10.2147/JPR.S557430

Immunofluorescence assays were performed to detect the protein expressions of EnSCs marker CD146, proliferation marker Ki-67, angiogenic marker molecule VEGF, and cell adhesion molecule ALCAM in the endometrium of normal mice and the ectopic endometrial tissue of EMS mice. The expression of CD146 was significantly increased in the EMS model group compared with the control group. Antibiotic treatment could suppress the expression of CD146. Moreover, adding sakuranin to antibiotic treatment could further enhance this effect (Figure 6A). Furthermore, Ki-67, VEGF, and ALCAM expression levels were considerably higher in the EMS group than in the other groups. Antibiotics markedly inhibited the expression of these molecules in EMS mice, and sakuranin further strengthened the effect of antibiotics (Figure 6B–D). Sakuranin significantly inhibits the pain level and EMT process of EMS in mice.

Sakuranin Enhances Sympathetic Neuron Markers and Inhibits Sensory Neuron Markers in EMS Mice

Ectopic endometrial implants are known to undergo sympathetic and sensory nerve innervation, contributing to peripheral neuroinflammation in endometriosis.[35] To investigate pain-related neural alterations, we performed tissue immunofluorescence analysis of pain-associated neuronal biomarkers, specifically the sympathetic nerve marker TH and the sensory nerve marker SP. The results revealed that in the EMS model group, the expression level of TH was significantly lower than that in the sham group, whereas the expression level of SP was significantly increased (Figure 6E). This suggested that in EMS, the number of sympathetic nerves decreased while the number of sensory nerves increased, which in turn influenced pain perception. After treatment with mixed antibiotics, the expression level of TH in EMS mice was increased, and SP was decreased. Significantly, in EMS mice treated with the combination of mixed antibiotics and sakuranin, the expression level of TH increased remarkably and even surpassed the level of the control group. Meanwhile, the expression level of SP was further decreased and was lower than that of the control group. These results demonstrated that sakuranin could enhance the number of sympathetic nerves and decrease the number of sensory nerves in ectopic lesions, thus reducing pain sensitivity.

Discussion

EMS is a multiple-clinical syndrome, and its pain symptoms cause significant suffering for many patients. The role of the gut microbiota in endometriosis-related pain is increasingly recognized.[36] However, the specific mechanisms by which GMRM affects the pain related to EMS are still unclear. Our study has identified sakuranin, a significant differential metabolite linked to the gut microbiota, which is downregulated in EMS patients with dysmenorrhea compared with those in EMS patients without dysmenorrhea and healthy controls. This metabolite exhibits a negative correlation with pain severity and may serve as a potential marker for the diagnosis of EMS and the assessment of pain. Furthermore, sakuranin may alleviate the progression of EMS and pain by potentially inhibiting the EnSCs differentiation, angiogenesis, inflammatory responses, and neuropathic pain (Figure 7). This study provides a new direction for the treatment of pain in EMS.

Studies have demonstrated that the metabolic characteristics of women with EMS have changed, with alterations observed in lipid metabolism, oxidative stress, inflammation, and other metabolic pathways.[37–40] However, the metabolite profiles associated with pain in EMS remain unrevealed. In our research on metabolomic profiling analysis, sakuranin, a significant differential metabolite between EMS patients with pain and non-pain controls, has drawn our attention. Sakuranin is the glycoside form of Sakuranetin, which is an active compound extracted from plants of the Prunus species and belongs to an important natural plant flavonoid. Flavonoids are a major class of natural products widely distributed in the plant kingdom. They are known for their properties such as cardioprotective, anticancer, antioxidant, anti-inflammatory, antiviral, antidiabetic, antimutagenic, and antibacterial[41] and are generally considered to have significant biological activity and pharmacological potential.[42–44] Daphne plants containing sakuranin are utilized in traditional medicine to treat joint pain and rheumatoid arthritis.[45,46] Additionally, we have also found that metabolic pathways such as steroid biosynthesis, vitamin B6 metabolism, riboflavin metabolism, Pantothenate and CoA biosynthesis exhibit significant differences among different groups. Y. Floman's research indicated that steroids could inhibit the synthesis and release of prostaglandins in inflammatory responses and are a well-known anti-inflammatory drug.[47]

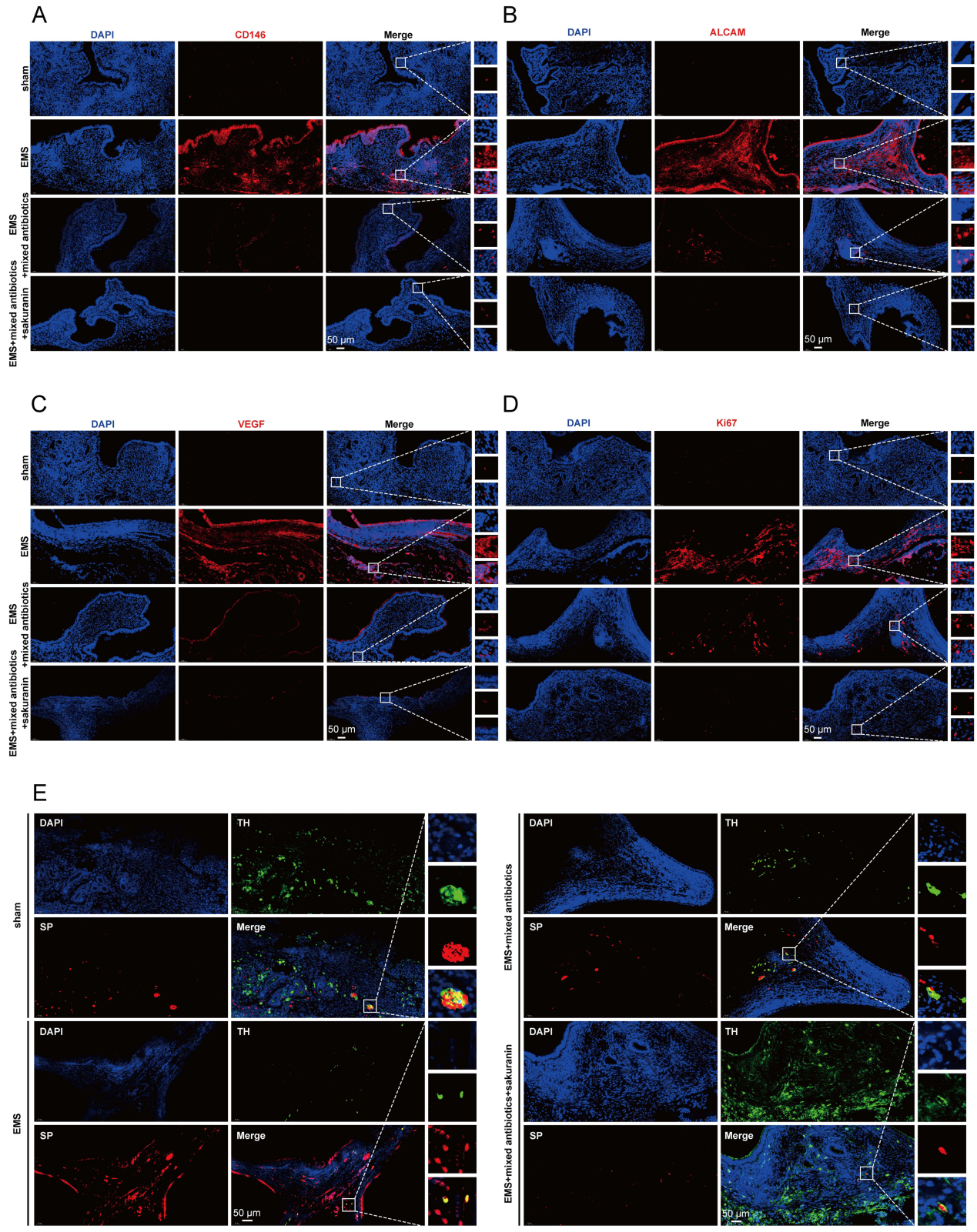

Figure 6 Immunofluorescence detection of protein expression in the endometrium of normal mice and the ectopic endometrial tissue of EMS mice. (**A**–**D**) Tissue immunofluorescence detection of the expressions of Cluster of differentiation 146 (CD146), ALCAM, VEGF, and Ki67 proteins. The expressions of the detected proteins are presented in red fluorescence, and the nuclear DAPI staining is shown in blue; (**E**) Tissue immunofluorescence detection of the expressions of tyrosine hydroxylase (TH) and the marker substance P (SP). Red represents the expression of SP protein, green represents the expression of TH protein, and blue represents the nuclear staining by DAPI.

https://doi.org/10.2147/JPR.S557430

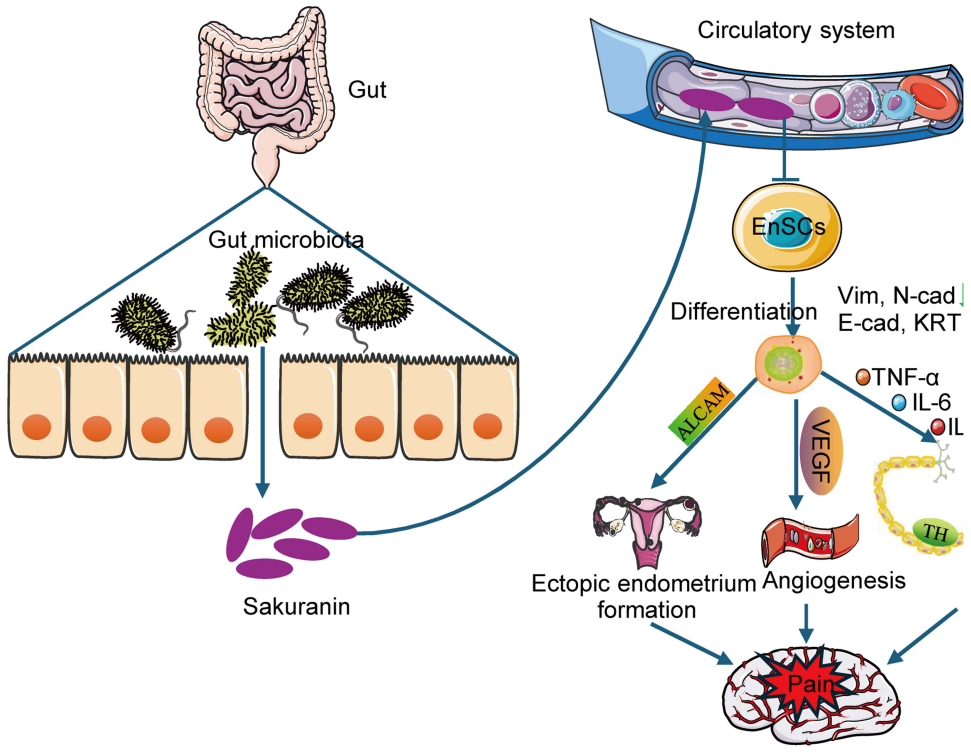

Figure 7 The molecular regulatory mechanism by which sakuranin mediates EnSCs to alleviate EMS-related pain. Blue arrows indicate the regulatory pathway of sakuranin on EnSCs; green arrows indicate decreased expression; red arrows indicate increased expression.
Abbreviations: Vim, vimentin; N-cad, N-cadherin; E-cad, E-cadherin; KRT10, cytokeratin 10; ALCAM, activated leukocyte cell adhesion molecule; VEGF, vascular endothelial growth factor; TNF-α, tumor necrosis factor-α; IL-6, interleukin-6; IL-1β, interleukin-1β; TH, tyrosine hydroxylase; SP, substance P. Figure adapted from Servier Medical Art.

Moreover, steroid metabolism and related pathways are closely associated with EMS, a hormone-dependent disease.[48,49] These findings suggest that the gut microbiota may affect the development of EMS through its metabolites and alleviate pain symptoms in EMS through multiple metabolic pathways, such as steroid synthesis.

Gut microbiota–derived metabolites play a pivotal role in host metabolism and disease regulation,[50] and dysbiosis is a hallmark of EMS. Painful EMS is characterized by an inflammatory microenvironment and estrogen imbalance, both of which disrupt intestinal homeostasis.[51,52] Such disturbances may suppress sakuranin-metabolizing symbionts, thereby reducing its bioavailability. Flavonoids, in particular, undergo extensive microbial biotransformation, with nearly 90% requiring enzymatic metabolism to enhance absorption.[53] Moreover, chronic pain–induced neuroendocrine stress and dysfunction of the brain–gut axis, which mediates bidirectional communication between the central nervous system and gastrointestinal tract, may further impair microbial metabolism.[54] Consistently, we observed an increased abundance of Prevotella, a genus linked to mucosal inflammation and systemic disease, alongside a decrease in Parabacteroides, reported to possess probiotic potential.[55,56] These microbial alterations provide a mechanistic rationale for the reduced levels of sakuranin and its associated taxa in painful EMS, potentially exacerbating local inflammation and enhancing pain perception.

EMS is regarded as an immune-related chronic inflammatory disease.[57] Elevated levels of pro-inflammatory factors such as IL-6, IL-1β, and TNF-α are closely associated with the pathological process of EMS.[58–60] Previous studies have shown that the abnormal expression of anti-inflammatory cytokines in EMS has a significant impact on its pathogenesis.[61–63] IL-6 is a major contributor to chronic inflammatory diseases and cytokine storms, and its role in inflammation cannot be overlooked. Additionally, inflammation is also one of the main causes of pain symptoms in EMS. The use of anti-inflammatory drugs can alleviate pain related to EMS.[61–63] Studies have shown that the disruption of the balance among sympathetic, parasympathetic, and sensory nerve functions, along with the misregulation of various cytokine secretions, can influence neurogenesis in EMS and initiate subsequent inflammatory reactions within the peripheral nervous system.[64] Peng et al's research pointed out that the expression of IL-1β in EMS lesions is related to severe deep dysmenorrhea.[65] In addition, norepinephrine, the main

neurotransmitter of the sympathetic nerve, can regulate the activity of immune cells and affect the levels of cytokines and antibodies such as TNF-α, IL-1β, interferon, adhesion molecules, and IL-6.[66] In our study, we found that the expression of the sympathetic nerve marker TH increased with sakuranin treatment. TH is a rate-limiting enzyme widely expressed in noradrenergic and dopaminergic neurons in the central nervous system.[67,68] At the same time, the expression of the sensory nerve marker SP was inhibited with sakuranin treatment. As a key neurotransmitter in the sensory nervous system, SP has a pro-inflammatory effect and can stimulate almost all immune cells,[69–71] and is a major contributor to neurogenic pain and inflammation.[70] In addition, the release of SP is regulated by the inflammatory factor IL-1β.[72]

EMS is a non-neoplastic invasive disease[73] and exhibits many characteristics similar to cancer.[74] EMT is a crucial step in the invasion process of tumor cells and plays a vital role in the pathogenesis of EMS. A significant feature of EMT is the decreased expression level of epithelial cell-specific markers alongside an increased expression of mesenchymal markers, which is directly related to the enhanced invasiveness of cells. In our study, we explored the phenotypic characteristics and epithelial-mesenchymal differentiation potential of cells by analyzing the expression of four markers: Vimentin, N-cadherin, E-cadherin, and Cytokeratin 10. Vimentin, as a key component of the cytoskeleton,[75] plays a crucial role in physiological processes such as cell migration, contraction, and proliferation,[76] and the absence of Vimentin will inhibit the differentiation ability of mesenchymal stem cells.[77]

Mesenchymal cadherin plays a crucial role in the differentiation process of mesenchymal cells. N-cadherin helps maintain the stemness of mesenchymal stem cells by mediating cell-cell adhesion and is highly expressed in mesenchymal cells. E-cadherin is essential for maintaining the pluripotency of embryonic stem cells and cell reprogramming.[78] As a marker of epithelial cell differentiation, Cytokeratin 10 is closely related to the specific differentiation state of cells.[79] The results of this study show that in EnSCs treated with sakuranin, the expression levels of E-cadherin and Cytokeratin 10 significantly increase, indicating that sakuranin may promote cell differentiation in the direction of epithelial characteristics. This change may weaken the migration and invasion ability of cells, thereby inhibiting the development of EMS. The Ki-67 index is a core marker for evaluating the cell proliferation state. Our results show that compared with non-EMS mice, EMS mice show higher proliferative activity. And sakuranin can inhibit the expression of Ki-67 in EMS mice, indicating that sakuranin may have the potential to inhibit the metastatic ability in the occurrence of EMS. Angiogenesis is a key factor in the occurrence process of EMS.[80–83] Studies have found that VEGF plays an important role in the occurrence and maintenance of peritoneal EMS,[84] and inhibiting the expression of VEGF can significantly inhibit the growth of endometriotic lesions.[85,86] This indicates that sakuranin treatment leads to a decrease in VEGF expression in ectopic lesions, indicating a reduction in angiogenesis in the lesions, and reducing the supply of oxygen and nutrients, which is not conducive to the maintenance of EMS lesions.

Beyond the inflammatory context, the potential roles of sakuranin in regulating the fate of normal EnSCs also merit consideration. Previous studies have reported that flavonoid compounds such as quercetin and naringenin can modulate cell cycle regulators, including p21 and Cyclin D1, thereby constraining excessive stem cell proliferation.[41,44] Although sakuranin at the tested concentrations did not show cytotoxicity in our experiments, it may act through similar mechanisms to balance proliferation and quiescence in normal EnSCs, preventing abnormal expansion under physiological conditions. In addition, flavonoids have been shown to enhance mitochondrial respiratory chain activity and suppress ROS generation.[41] Given that the metabolic state of EnSCs critically shapes their differentiation potential, sakuranin may indirectly influence their cell fate decisions by maintaining metabolic and redox homeostasis. These possible roles in normal EnSCs expand the biological significance of sakuranin and warrant further mechanistic investigation.

Our study is subject to several limitations. Firstly, the relatively small sample size, a consequence of the stringent inclusion criteria, limits the generalizability of our findings and underscores the need for validation in larger cohorts. Secondly, while this study identified an association between sakuranin and the gut microbiota, causal relationships and interaction mechanisms remain unclear. Future studies using fecal microbiota transplantation or selective microbial colonization could elucidate dynamic interactions within the gut microbiota-sakuranin-endometriosis axis. Thirdly, the cross-sectional nature of our design precludes the establishment of causal relationships between sakuranin levels and pain dynamics. Longitudinal studies are requisite to ascertain causality. Fourth, notwithstanding the demonstrated efficacy of sakuranin in preclinical models, its translational pertinence to human pathophysiology necessitates further pharmacokinetic and safety appraisals. Moreover, forthcoming research will probe into the molecular mechanisms underpinning the impact of sakuranin on EMS-associated pain.

Conclusion

In conclusion, based on the metabolomic profiling and experimental analyses conducted in this study, we have drawn the metabolic atlas of patients with EMS-related pain and identified differential metabolites and differential signaling pathways between EMS patients with and without pain. Among these, sakuranin can inhibit endometrial stem cell transformation, reduce inflammation and angiogenesis, and modulate nerve-related marker expression, which together contributed to alleviating EMS-associated pain. Although the sample size was limited, these results offer preliminary evidence supporting sakuranin as a potential therapeutic strategy for EMS-related pain, warranting further validation in larger cohorts.

Data Sharing Statement

The dataset is available from the corresponding author upon reasonable request.

Ethical Approval

The study was approved by the Ethics Committee of The Sixth Affiliated Hospital of Sun Yat-sen University (human study approval number: 2024ZSLYEC-020; animal study approval number: BG-001-R3).

Informed Consent Statement

Written informed consent was obtained from all the participants.

Author Contributions

All authors made a significant contribution to the work reported, whether that is in the conception, study design, execution, acquisition of data, analysis and interpretation, or in all these areas; took part in drafting, revising or critically reviewing the article; gave final approval of the version to be published; have agreed on the journal to which the article has been submitted; and agree to be accountable for all aspects of the work.

Funding

This research was supported by a project from The Sixth Affiliated Hospital of Sun Yat-sen University's Clinical Medical Research Program (project number: 2022A1515012401).

Disclosure

The authors report no conflicts of interest in this work.

References

1. Bulun SE. Endometriosis. *N Engl J Med*. 2009;360(3):268–279. doi:10.1056/NEJMra0804690
2. Khine YM, Taniguchi F, Harada T. Clinical management of endometriosis-associated infertility. *Reprod Med Biol*. 2016;15(4):217–225. doi:10.1007/s12522-016-0237-9
3. Sachedina A, Todd N. Dysmenorrhea, Endometriosis and Chronic Pelvic Pain in Adolescents. *J Clin Res Pediatr Endocrinol*. 2020;12(Suppl 1):7–17. doi:10.4274/jcrpe.galenos.2019.2019.S0217
4. Berkley KJ, Dmitrieva N, Curtis KS, Papka RE. Innervation of ectopic endometrium in a rat model of endometriosis. *Proc Natl Acad Sci U S A*. 2004;101(30):11094–11098. doi:10.1073/pnas.0403663101
5. Alvarez P, Chen X, Hendrich J, et al. Ectopic uterine tissue as a chronic pain generator. *Neuroscience*. 2012;225:269–282. doi:10.1016/j.neuroscience.2012.08.033
6. McAllister SL, Dmitrieva N, Berkley KJ. Sprouted innervation into uterine transplants contributes to the development of hyperalgesia in a rat model of endometriosis. *PLoS One*. 2012;7(2):e31758. doi:10.1371/journal.pone.0031758
7. Aich A, Afrin LB, Gupta K. Mast cell-mediated mechanisms of nociception. *Int J Mol Sci*. 2015;16(12):29069–29092. doi:10.3390/ijms161226151
8. Tran LV, Tokushige N, Berbic M, Markham R, Fraser IS. Macrophages and nerve fibres in peritoneal endometriosis. *Hum Reprod*. 2009;24(4):835–841. doi:10.1093/humrep/den483
9. Van Langendonckt A, Casanas-Roux F, Donnez J. Oxidative stress and peritoneal endometriosis. *Fertil Steril*. 2002;77(5):861–870. doi:10.1016/s0015-0282(02)02959-x
10. Ferrero S, Haas S, Remorgida V, et al. Loss of sympathetic nerve fibers in intestinal endometriosis. *Fertil Steril*. 2010;94(7):2817–2819. doi:10.1016/j.fertnstert.2010.06.069

11. Alonso A, Gunther K, Maheux-Lacroix S, Abbott J. Medical management of endometriosis. *Curr Opin Obstet Gynecol*. 2024;36(5):353–361. doi:10.1097/gco.0000000000000983
12. Vercellini P, Buggio L, Frattaruolo MP, Borghi A, Dridi D, Somigliana E. Medical treatment of endometriosis-related pain. *Best Pract Res Clin Obstet Gynaecol*. 2018;51:68–91. doi:10.1016/j.bpobgyn.2018.01.015
13. Leyendecker G, Herbertz M, Kunz G, Mall G. Endometriosis results from the dislocation of basal endometrium. *Hum Reprod*. 2002;17 (10):2725–2736. doi:10.1093/humrep/17.10.2725
14. Starzinski-Powitz A, Zeitvogel A, Schreiner A, Baumann R. In search of pathogenic mechanisms in endometriosis: the challenge for molecular cell biology. *Curr Mol Med*. 2001;1(6):655–664. doi:10.2174/1566524013363168
15. Gargett CE. Uterine stem cells: what is the evidence? *Hum Reprod Update*. 2007;13(1):87–101. doi:10.1093/humupd/dml045
16. Gargett CE, Schwab KE, Deane JA. Endometrial stem/progenitor cells: the first 10 years. *Hum Reprod Update*. 2016;22(2):137–163. doi:10.1093/humupd/dmv051
17. Zhang X, Zhao G, Hu Y. Advancements in endometrial epithelial stem cell research. *Sci China Life Sci*. 2022;65(1):215–218. doi:10.1007/s11427-021-1988-1
18. Canosa S, Moggio A, Brossa A, et al. Angiogenic properties of endometrial mesenchymal stromal cells in endothelial co-culture: an in vitro model of endometriosis. *Mol Hum Reprod*. 2017;23(3):187–198. doi:10.1093/molehr/gax006
19. Kao AP, Wang KH, Chang CC, et al. Comparative study of human eutopic and ectopic endometrial mesenchymal stem cells and the development of an in vivo endometriotic invasion model. *Fertil Steril*. 2011;95(4):1308–15.e1. doi:10.1016/j.fertnstert.2010.09.064
20. Li J, Dai Y, Zhu H, Jiang Y, Zhang S. Endometriotic mesenchymal stem cells significantly promote fibrogenesis in ovarian endometrioma through the Wnt/β-catenin pathway by paracrine production of TGF-β1 and Wnt1. *Hum Reprod*. 2016;31(6):1224–1235. doi:10.1093/humrep/dew058
21. Koippallil Gopalakrishnan Nair AR, Pandit H, Warty N, Madan T. Endometriotic mesenchymal stem cells exhibit a distinct immune phenotype. *Int Immunol*. 2015;27(4):195–204. doi:10.1093/intimm/dxu103
22. Talwar C, Singh V, Kommagani R. The gut microbiota: a double-edged sword in endometriosis†. *Biol Reprod*. 2022;107(4):881–901. doi:10.1093/biolre/ioac147
23. Salliss ME, Farland LV, Mahnert ND, Herbst-Kralovetz MM. The role of gut and genital microbiota and the estrobolome in endometriosis, infertility and chronic pelvic pain. *Hum Reprod Update*. 2021;28(1):92–131. doi:10.1093/humupd/dmab035
24. Chadchan SB, Popli P, Ambati CR, et al. Gut microbiota-derived short-chain fatty acids protect against the progression of endometriosis. *Life Sci Alliance*. 2021;4(12). doi:10.26508/lsa.202101224
25. Ni Z, Sun S, Bi Y, et al. Correlation of fecal metabolomics and gut microbiota in mice with endometriosis. *Am J Reprod Immunol*. 2020;84(6): e13307. doi:10.1111/aji.13307
26. Allaire C, Bedaiwy MA, Yong PJ. Diagnosis and management of endometriosis. *Cmaj*. 2023;195(10):E363–e371. doi:10.1503/cmaj.220637
27. Ma D, Zhu Z, Tan X, et al. Validation of peripheral neuromodulation mechanisms of icariin in knee osteoarthritis-related chronic pain. *J Cell Mol Med*. 2024;28(23):e70223. doi:10.1111/jcmm.70223
28. Yang Y, Qu JY, Guo H, et al. Electroacupuncture at sensitized acupoints relieves somatic referred pain in colitis rats by inhibiting sympathetic-sensory coupling to interfere with 5-HT signaling pathway. *Chin J Integr Med*. 2024;30(2):152–162. doi:10.1007/s11655-023-3565-8
29. Lu F, Wei J, Zhong Y, et al. Antibiotic therapy and vaginal microbiota transplantation reduce endometriosis disease progression in female mice via NF-κB signaling pathway. *Front Med Lausanne*. 2022;9:831115. doi:10.3389/fmed.2022.831115
30. Chadchan SB, Cheng M, Parnell LA, et al. Antibiotic therapy with metronidazole reduces endometriosis disease progression in mice: a potential role for gut microbiota. *Human Reproduction*. 2019;34(6):1106–1116. doi:10.1093/humrep/dez041
31. Muraoka A, Suzuki M, Hamaguchi T, et al. Fusobacterium infection facilitates the development of endometriosis through the phenotypic transition of endometrial fibroblasts. *Sci Transl Med*. 2023;15(700):eadd1531. doi:10.1126/scitranslmed.add1531
32. Shi W, Wang M, Jin Z, et al. Deciphering the pain-related gut microbiome in patients with endometriosis. *CEOG*. 2025;52(11). doi:10.31083/ceog45531
33. Kitawaki J, Ishihara H, Koshiba H, et al. Usefulness and limits of CA-125 in diagnosis of endometriosis without associated ovarian endometriomas. *Hum Reprod*. 2005;20(7):1999–2003. doi:10.1093/humrep/deh890
34. Karli P. The relationship of pelvic pain symptoms with CA-125 levels in endometriosis cases. *Ann Med Res*. 2019;26(7).
35. Wei Y, Liang Y, Lin H, Dai Y, Yao S. Autonomic nervous system and inflammation interaction in endometriosis-associated pain. *J Neuroinflammation*. 2020;17(1):80. doi:10.1186/s12974-020-01752-1
36. Coxon L, Demetriou L, Vincent K. Current developments in endometriosis-associated pain. *Cell Rep Med*. 2024;5(10):101769. doi:10.1016/j.xcrm.2024.101769
37. Dutta M, Joshi M, Srivastava S, Lodh I, Chakravarty B, Chaudhury K. A metabonomics approach as a means for identification of potential biomarkers for early diagnosis of endometriosis. *Mol Biosyst*. 2012;8(12):3281–3287. doi:10.1039/c2mb25353d
38. Murgia F, Angioni S, D'Alterio MN, et al. Metabolic profile of patients with severe endometriosis: a prospective experimental study. *Reprod Sci*. 2021;28(3):728–735. doi:10.1007/s43032-020-00370-9
39. Jana SK, Dutta M, Joshi M, Srivastava S, Chakravarty B, Chaudhury K. 1H NMR based targeted metabolite profiling for understanding the complex relationship connecting oxidative stress with endometriosis. *Biomed Res Int*. 2013;2013:329058. doi:10.1155/2013/329058
40. Dutta M, Singh B, Joshi M, et al. Metabolomics reveals perturbations in endometrium and serum of minimal and mild endometriosis. *Sci Rep*. 2018;8(1):6466. doi:10.1038/s41598-018-23954-7
41. Stompor M. A review on sources and pharmacological aspects of Sakuranetin. *Nutrients*. 2020;12(2). doi:10.3390/nu12020513
42. Vazhappilly CG, Amararathna M, Cyril AC, et al. Current methodologies to refine bioavailability, delivery, and therapeutic efficacy of plant flavonoids in cancer treatment. *J Nutr Biochem*. 2021;94:108623. doi:10.1016/j.jnutbio.2021.108623
43. Hazafa A, Rehman KU, Jahan N, Jabeen Z. The role of polyphenol (flavonoids) compounds in the treatment of cancer cells. *Nutr Cancer*. 2020;72 (3):386–397. doi:10.1080/01635581.2019.1637006
44. Breinholt V, Lauridsen ST, Dragsted LO. Differential effects of dietary flavonoids on drug metabolizing and antioxidant enzymes in female rat. *Xenobiotica*. 1999;29(12):1227–1240. doi:10.1080/004982599237903
45. Zhang CF, Zhang SL, He X, et al. Antioxidant effects of Genkwa flos flavonoids on Freund's adjuvant-induced rheumatoid arthritis in rats. *J Ethnopharmacol*. 2014;153(3):793–800. doi:10.1016/j.jep.2014.03.046

46. Jiang CP, He X, Yang XL, et al. Anti-rheumatoid arthritic activity of flavonoids from Daphne genkwa. *Phytomedicine*. 2014;21(6):830–837. doi:10.1016/j.phymed.2014.01.009
47. Popescu LM. Anti-inflammatory agents-steroids as anti-inflammatory agents. In: *Pharmacology of the Eye*. 2011.
48. Zhao Y, Gong P, Chen Y, et al. Dual suppression of estrogenic and inflammatory activities for targeting of endometriosis. *Sci Transl Med*. 2015;7 (271):271ra9. doi:10.1126/scitranslmed.3010626
49. Greene AD, Lang SA, Kendziorski JA, Sroga-Rios JM, Herzog TJ, Burns KA. Endometriosis: where are we and where are we going? *Reproduction*. 2016;152(3):R63–78. doi:10.1530/rep-16-0052
50. Brown EM, Clardy J, Xavier RJ. Gut microbiome lipid metabolism and its impact on host physiology. *Cell Host Microbe*. 2023;31(2):173–186. doi:10.1016/j.chom.2023.01.009
51. Yu J, Berga SL, Zou E, et al. Neurotrophins and their receptors, novel therapeutic targets for pelvic pain in endometriosis, are coordinately regulated by IL-1β via the JNK signaling pathway. *Am J Pathol*. 2023;193(8):1046–1058. doi:10.1016/j.ajpath.2023.04.007
52. Li Z, Yin Z, Chen W, Wang Z. Impact of gut and reproductive tract microbiota on estrogen metabolism in endometriosis. *Am J Reprod Immunol*. 2025;93(6):e70109. doi:10.1111/aji.70109
53. Al-Ishaq RK, Liskova A, Kubatka P, Büsselberg D. Enzymatic metabolism of flavonoids by gut microbiota and its impact on gastrointestinal cancer. *Cancers (Basel)*. 2021;13(16). doi:10.3390/cancers13163934
54. Ho T, Elma Ö, Kocanda L, et al. The brain-gut axis and chronic pain: mechanisms and therapeutic opportunities. *Front Neurosci*. 2025;19:1545997. doi:10.3389/fnins.2025.1545997
55. Larsen JM. The immune response to Prevotella bacteria in chronic inflammatory disease. *Immunology*. 2017;151(4):363–374. doi:10.1111/imm.12760
56. Liu J, Qiu H, Zhao J, et al. Parabacteroides as a promising target for disease intervention: current stage and pending issues. *NPJ Biofilms Microbiomes*. 2025;11(1):137. doi:10.1038/s41522-025-00772-0
57. Riccio L, Santulli P, Marcellin L, Abrão MS, Batteux F, Chapron C. Immunology of endometriosis. *Best Pract Res Clin Obstet Gynaecol*. 2018;50:39–49. doi:10.1016/j.bpobgyn.2018.01.010
58. Symons LK, Miller JE, Tyryshkin K, et al. Neutrophil recruitment and function in endometriosis patients and a syngeneic murine model. *FASEB J*. 2020;34(1):1558–1575. doi:10.1096/fj.201902272R
59. Martínez S, Garrido N, Coperias JL, et al. Serum interleukin-6 levels are elevated in women with minimal-mild endometriosis. *Hum Reprod*. 2007;22(3):836–842. doi:10.1093/humrep/del419
60. Cho SH, Oh YJ, Nam A, et al. Evaluation of serum and urinary angiogenic factors in patients with endometriosis. *Am J Reprod Immunol*. 2007;58 (6):497–504. doi:10.1111/j.1600-0897.2007.00535.x
61. Zhou WJ, Yang HL, Shao J, et al. Anti-inflammatory cytokines in endometriosis. *Cell Mol Life Sci*. 2019;76(11):2111–2132. doi:10.1007/s00018-019-03056-x
62. Sharpe-Timms KL, Nabli H, Zimmer RL, Birt JA, Davis JW. Inflammatory cytokines differentially up-regulate human endometrial haptoglobin production in women with endometriosis. *Hum Reprod*. 2010;25(5):1241–1250. doi:10.1093/humrep/deq032
63. Jiang L, Yan Y, Liu Z, Wang Y. Inflammation and endometriosis. *Front Biosci*. 2016;21(5):941–948. doi:10.2741/4431
64. Wu J, Xie H, Yao S, Liang Y. Macrophage and nerve interaction in endometriosis. *J Neuroinflammation*. 2017;14(1):53. doi:10.1186/s12974-017-0828-3
65. Peng B, Alotaibi FT, Sediqi S, Bedaiwy MA, Yong PJ. Role of interleukin-1β in nerve growth factor expression, neurogenesis and deep dyspareunia in endometriosis. *Hum Reprod*. 2020;35(4):901–912. doi:10.1093/humrep/deaa017
66. Kin NW, Sanders VM. It takes nerve to tell T and B cells what to do. *J Leukoc Biol*. 2006;79(6):1093–1104. doi:10.1189/jlb.1105625
67. Levitt M, Spector S, Sjoerdsma A, Udenfriend S. Elucidation of the rate-limiting step in norepinephrine biosynthesis in the perfused Guinea-pig heart. *J Pharmacol Exp Ther*. 1965;148:1–8.
68. Nagatsu T, Levitt M, Udenfriend S. Tyrosine hydroxylase. the initial step in norepinephrine biosynthesis. *J Biol Chem*. 1964;239:2910–2917.
69. Jancsó N, Jancsó-Gábor A, Szolcsányi J. Direct evidence for neurogenic inflammation and its prevention by denervation and by pretreatment with capsaicin. *Br J Pharmacol Chemother*. 1967;31(1):138–151. doi:10.1111/j.1476-5381.1967.tb01984.x
70. Schmidt MJ, Roth J, Ondreka N, Kramer M, Rummel C. A potential role for substance P and interleukin-6 in the cerebrospinal fluid of Cavalier King Charles Spaniels with neuropathic pain. *J Vet Intern Med*. 2013;27(3):530–535. doi:10.1111/jvim.12080
71. Levine JD, Clark R, Devor M, Helms C, Moskowitz MA, Basbaum AI. Intraneuronal substance P contributes to the severity of experimental arthritis. *Science*. 1984;226(4674):547–549. doi:10.1126/science.6208609
72. Barnes PJ, Baraniuk JN, Belvisi MG. Neuropeptides in the respiratory tract. Part I. *Am Rev Respir Dis*. 1991;144(5):1187–1198. doi:10.1164/ajrccm/144.5.1187
73. Zeitvogel A, Baumann R, Starzinski-Powitz A. Identification of an invasive, N-cadherin-expressing epithelial cell type in endometriosis using a new cell culture model. *Am J Pathol*. 2001;159(5):1839–1852. doi:10.1016/s0002-9440(10)63030-1
74. Chui MH, Wang TL, Shih IM. Endometriosis: benign, malignant, or something in between? *Oncotarget*. 2017;8(45):78263–78264. doi:10.18632/oncotarget.21051
75. Premchandar A, Mücke N, Poznański J, et al. Structural dynamics of the vimentin coiled-coil contact regions involved in filament assembly as revealed by hydrogen-deuterium exchange. *J Biol Chem*. 2016;291(48):24931–24950. doi:10.1074/jbc.M116.748145
76. Rogel MR, Soni PN, Troken JR, Sitikov A, Trejo HE, Ridge KM. Vimentin is sufficient and required for wound repair and remodeling in alveolar epithelial cells. *FASEB J*. 2011;25(11):3873–3883. doi:10.1096/fj.10-170795
77. Wang K, Du B, Zhang Y, et al. Vimentin-Rab7a Pathway Mediates the Migration of MSCs and Lead to Therapeutic Effects on ARDS. *Stem Cells Int*. 2021;2021:9992381. doi:10.1155/2021/9992381
78. Redmer T, Diecke S, Grigoryan T, Quiroga-Negreira A, Birchmeier W, Besser D. E-cadherin is crucial for embryonic stem cell pluripotency and can replace OCT4 during somatic cell reprogramming. *EMBO Rep*. 2011;12(7):720–726. doi:10.1038/embor.2011.88
79. Fuchs E. Keratins as biochemical markers of epithelial differentiation. *Trends Genet*. 1988;4(10):277–281. doi:10.1016/0168-9525(88)90169-2
80. Porpora MG, Scaramuzzino S, Sangiuliano C, et al. High prevalence of autoimmune diseases in women with endometriosis: a case-control study. *Gynecol Endocrinol*. 2020;36(4):356–359. doi:10.1080/09513590.2019.1655727

81. Young VJ, Brown JK, Saunders PT, Horne AW. The role of the peritoneum in the pathogenesis of endometriosis. *Hum Reprod Update*. 2013;19 (5):558–569. doi:10.1093/humupd/dmt024
82. Lin YH, Chen YH, Chang HY, Au HK, Tzeng CR, Huang YH. Chronic niche inflammation in endometriosis-associated infertility: current understanding and future therapeutic strategies. *Int J Mol Sci*. 2018;19(8). doi:10.3390/ijms19082385
83. Greenbaum H, Weil C, Chodick G, Shalev V, Eisenberg VH. Evidence for an association between endometriosis, fibromyalgia, and autoimmune diseases. *Am J Reprod Immunol*. 2019;81(4):e13095. doi:10.1111/aji.13095
84. McLaren J. Vascular endothelial growth factor and endometriotic angiogenesis. *Hum Reprod Update*. 2000;6(1):45–55. doi:10.1093/humupd/6.1.45
85. Liu S, Xin X, Hua T, et al. Efficacy of anti-VEGF/VEGFR agents on animal models of endometriosis: a systematic review and meta-analysis. *PLoS One*. 2016;11(11):e0166658. doi:10.1371/journal.pone.0166658
86. Streuli I, Santulli P, Chouzenoux S, Chapron C, Batteux F. Serum osteopontin levels are decreased in focal adenomyosis. *Reprod Sci*. 2017;24 (5):773–782. doi:10.1177/1933719116669054